

1 Accepted in “Geological Journal” (Wiley)

2

3 **Study of Coal-Bearing Heterolithic Units for Reconstructing**
 4 **Marine Pathways in the Eastern Gondwana Basin, India**

5

6 Manish Kumar Srivastava¹, Kaushal Kishor¹, Alok K. Singh^{1*}, Shivranjan Kumar
 7 Bharti² and Soumyajit Mukherjee³

8

9 ¹ Department of Petroleum Engineering and Geoengineering, Rajiv Gandhi Institute of
 10 Petroleum Technology, Jais 229304, Amethi, Uttar Pradesh, INDIA

11

12 ² State Unit Jharkhand, Geological Survey of India, Ranchi 834002, Jharkhand, INDIA

13

14 ³ Department of Earth Sciences, Indian Institute of Technology Bombay, Powai, Mumbai
 15 400076, Maharashtra, INDIA
 16 asingh@rgipt.ac.in

17 **Abstract**

18 The Gondwana sequence has traditionally been viewed as resulting from post-glacial fluvio-
 19 lacustrine sedimentation within large, elongated rift valleys during the Permian Period. However,
 20 doubts have recently been raised regarding its freshwater origin. This research fills that gap
 21 through a multidisciplinary approach-incorporating sedimentological study, coal petrography,
 22 mineralogy and major and trace element geochemistry demonstrating a dynamic depositional
 23 environment controlled by tidal, wave and river interactions. Geochemical proxies viz., CaO/MgO,
 24 Sr/Ba, and Th/U ratios, along with MgO and Al₂O₃ trends, reveal fluctuating paleo-salinity
 25 conditions from brackish to marine environment. The presence of dolomite, siderite, limited pyrite
 26 and alginite macerals further confirms episodic marine influence during peat formation.
 27 Heterolithic units, the principal sedimentary facies in the study area, archives tidal bundles,
 28 coarsening-upward successions, and wave-ripple-tidalite features, indicative of deposition across
 29 supratidal to subtidal salt marsh settings. The coal-bearing heterolithic units form during multiple
 30 minor marine transgressions. A regressive shift is marked by the deposition of the Dumerbera and
 31 Parsatoli Sandstone units, followed by a major transgression that initiated the ironstone-rich Barren
 32 Measure Formation. These transgressions predate the previously documented marine inundation
 33 of the overlying Barren Measures Formation, implying that marginal marine conditions developed
 34 earlier in this basin than previously thought. This study provides clear evidence of marine influence

35 during Barakar sedimentation and supports the existence of a near-continuous marine incursion
36 pathway from the Khemgaon–Sikkim corridor to the Satpura Basin, reflecting sustained marine
37 connectivity across Gondwana basins. By refining the regional paleoenvironmental model of
38 Indian Gondwana, this study emphasizes the efficacy of multi-proxy frameworks in decoding
39 complex depositional systems.

40 **Keywords:** Barakar Formation, Gondwana marine incursion, Heterolithic units, Trace element
41 geochemistry, West Bokaro basin.

42 **Statement and Declarations:**

43 **Availability of data and materials**– Data can be provided as needed.

44 **Competing Interests**– We hereby confirm that there are no financial or other conflicts of interest
45 associated with the submission of this paper.

46 **Funding**– Current research was conducted without any external funding.

47 **Author's Contributions**– MKS, SKB, KK and AKS contributed to the analysis and interpretation
48 of the results. MKS and SB conducted field work, AKS provided supervision, and MKS, SKB,
49 KK, SM and AKS worked on the initial manuscript draft, while AKS and SM revised it. All authors
50 reviewed the findings and gave their approval for the final draft of the manuscript.

51 **Acknowledgments**– The director of the Rajiv Gandhi Institute of Petroleum Technology (RGIFT),
52 Jais, Amethi, Uttar Pradesh, India, is thanked for providing the required resources.

53 **1 Introduction**

54 Rifting of Gondwanaland during the Late Carboniferous to Early Permian period developed
55 several intracratonic rift basins filled with continental clastic deposits (Mathews et al. 2020). A
56 long episode (Permo-Carboniferous to Early Cretaceous) of fluvial sedimentation, took place in
57 such rift basins (Tewari and Maejima 2010). All such sediments are grouped under stratigraphic
58 framework as The Gondwana Supergroup. Several of these sediment layers are renowned for their
59 rich fossil flora and fauna, as well as economically exploitable coal seams.

60 The Permian coal-bearing sediments of India has traditionally been marked as fluvio-lacustrine
61 depositional system, based on sedimentological study and non-availability of marine fossils

62 (Casshyap 1987; Ray and Chakraborty 2002; Tewari et al. 2012) and many more, however, many
63 researchers (Goswami 2008; Bhattacharya et al. 2021) also encountered the sign of marine
64 intrusions during their deposition. The marine origin of the Barakar Formation has been a
65 longstanding topic of debate across the Gondwana rift.

66 The initial identification of a marine signature within the predominantly non-marine Gondwana
67 Sequence was made based on the *Eurydesma-Productus-Conularia* assemblage in the Umaria
68 Marine Bed, as reported by Sinor in 1923 (Goswami 2008). Chatterjee and Hotton (1986) proposed
69 that a large-scale marine transgression occurred through Gondwana rift system, in peninsular India
70 during the lower Permian, as part of their paleogeographic reconstruction work (Chatterjee and
71 Hotton 1986). Subsequently, the marine nature of the Gondwana sediments is also confirmed by
72 the presence of invertebrate fossils from Manendragrah (Chhattisgarh), Daltonganj (Jharkhand),
73 Rajhara (Jharkhand), Ranjit Pebble Slate (Sikkim), Subansiri (Arunachal Pradesh), and Bap
74 Boulder Bed (Rajasthan) (Figure 1) (Venkatachala and Tiwari 1987; Goswami 2008). Most of
75 these sediments also contain acritarchs, leiosphaerids and other palynofossils of marine origin in
76 association with spores and pollen (Venkatachala and Tiwari 1987).

77 The Gondwana sedimentation began with the deposition of the Talchir Formation, whose marine
78 nature is already well established (Venkatachala and Tiwari 1987). Interestingly, recent studies
79 across various Gondwana basins of India have increasingly highlighted the role of marine
80 influence during the deposition of the Barakar Formation as well (Table 1). Multiple Gondwana
81 basins of India, including Rajmahal, Raniganj, West Bokaro, South Karanpura, Rajhara, Ib River,
82 Talcher and Satpura exhibit compelling evidence of marine influence during the Barakar
83 Formation sedimentation, as indicated by sedimentological, ichnological, palynological, and
84 geochemical data (Gupta 1999; Chakraborty et al. 2003; Ghosh et al. 2004; Goswami 2008;
85 Bhattacharjee et al. 2018; Mathews et al. 2020; Bhattacharya et al. 2021, 2012a; Pillai et al. 2023).
86 These findings collectively suggest that post-glacial sea-level rise led to episodic to sustained
87 marine incursions, resulting in estuarine to peritidal depositional settings across these coal-bearing
88 basins. Recently, the signatures of Permian Tethyan transgression were recorded from Barren
89 Measures Formation, West Bokaro Coalfield (Bhattacharya and Banerjee 2015). Thus, the
90 previous view of predominantly non-marine origin of Lower Gondwana has been challenged.

91 **Table 1:** Summary of marine influence and depositional settings of the Barakar Formation across
 92 various Gondwana basins of India, highlighting evidence from sedimentological, ichnological, and
 93 geochemical indicators as reported in previous studies.

Location	Depositional setting	Reference
Raniganj Basin, West Bengal	Barakar Formation experienced a significant marine incursion, likely due to post-glacial sea-level rise during the Permian. This transgressive event led to the development of estuarine conditions.	(Bhattacharjee et al. 2018; Bhattacharya et al. 2021, 2012b)
Ib river valley and Talcher Basin, Orissa	The presence of sparry calcite cementation, phosphate-bearing peloids, marine ichnotaxa, bioturbated beds, and brackish-water palynofossils in the Barakar Formation strongly supports episodic marine incursions during its sedimentation in the Ib River and Talcher basins.	(Goswami 2008)
Satpura basin, Madhya Pradesh	The Barakar Formation in the Satpura Basin, once considered purely continental, is now reinterpreted as having formed in a tidally influenced deltaic setting. Evidence such as bidirectional cross-strata and tidal rhythmites suggests significant marine influence, highlighting a tidal estuarine environment and revising earlier palaeogeographic models of Gondwanan coal basins.	(Ghosh et al. 2004)
Mohpani Coalfield, Satpura Gondwana Basin, Madhya Pradesh	This study reveals clear evidence of marine incursion during Barakar Formation sedimentation, with tidal signatures identified in mudstone-dominated facies. Features such as flaser bedding, spring-neap tidal cycles, bidirectional foresets, and desiccation cracks indicate deposition in intertidal to supratidal environments, challenging the earlier view of a purely continental braided river system and confirming significant marine influence.	(Chakraborty et al. 2003)
Ramgarh, South Karanpura, and West Bokaro coalfields, Jharkhand	Marine influence in the Barakar Formation has been identified based on trace fossils, sedimentary features, and trace element content. The upper part indicates deposition in a peritidal setting near a broad, shallow epicontinental sea, with storm activity playing a key role during high sea-level conditions.	(Gupta 1999)

Rajhara Coalfeld, Palamu, Jharkhand	Geochemical signatures suggest a brackish palaeoenvironment prevailed during the Late Permian (Artinskian) in the Rajhara Colliery.	(Pillai et al. 2023)
--	---	----------------------

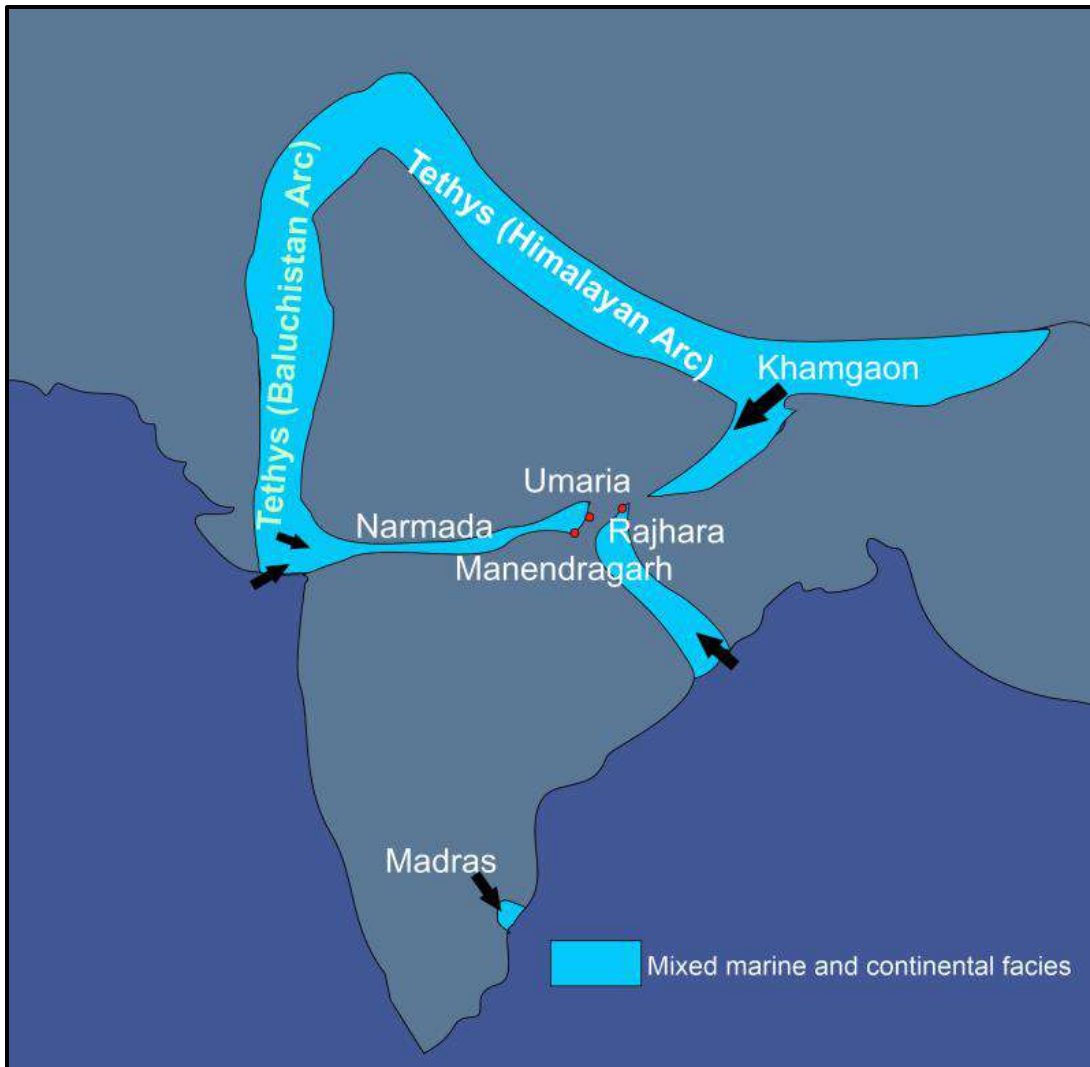
94

95 **1.1 Necessity of research**

96 From the studies reporting marine incursion during the Early Permian, it seems that nearly all the
 97 low-lying embryonic basinal depressions experienced marine transgression from an eastern bay.
 98 In the west and northwest, these marine pathways connected with the Arabian Sea and the Salt
 99 Range Sea (Chatterjee and Hotton 1986). Evidence of episodic marine transgression into the
 100 Middle and Late Permian in central India further necessitates the search for such signatures to
 101 establish the remnants of these pathways inside the peninsula. The Bokaro basin is one such gap
 102 where marine signatures have yet to be confirmed by multi-proxy tools.

103 Multi-proxy studies are crucial in sedimentary depositional environment research because they
 104 provide a more comprehensive and detailed understanding of past environmental conditions
 105 compared to single-proxy approaches. By combining multiple lines of evidence from different
 106 proxies, the limitations of individual proxies can be overcome and gain a more nuanced picture of
 107 past environmental changes (Birks and Birks 2006; Schroeter et al. 2020; Quamar et al. 2024).

108 In this study, we attempt to evaluate the paleo-salinity conditions, ichnofossils, paleo-depositional
 109 environment, of sandstone–mudstone heteroliths, coal, and claystone of the Early Permian Barakar
 110 Formation in the West Bokaro Basin, using sedimentology, organic micropetrographic analysis,
 111 and major and trace element geochemistry. Connection with Tethys was established through the
 112 same pathways as Early Sakmarian (Mukhopadhyay et al. 2010). By confirming the marine origin
 113 of the Barakar Formation in the West Bokaro Basin, this study aims to connect the missing links
 114 between the eastern and western marine pathways and contribute to a re-evaluation of Gondwana
 115 palaeogeography. The analysis will provide a detailed assessment of the paleo-depositional
 116 conditions of the Barakar Formation and reveal the extent of Permian marine inundations in eastern
 117 India.

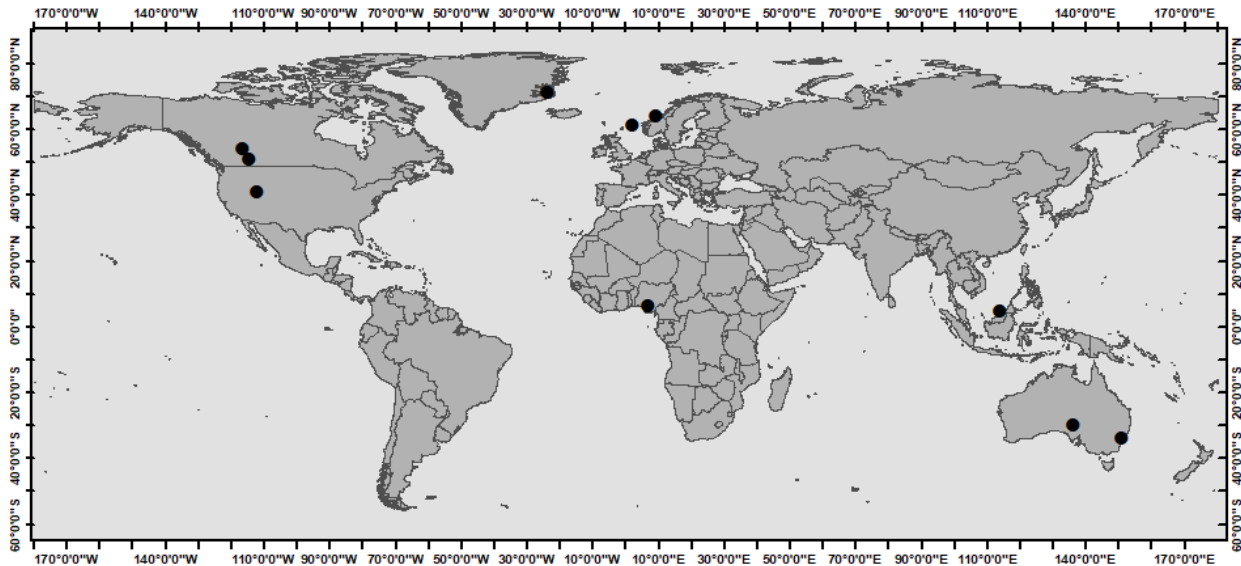


118

119 **Figure 1:** Cartoon Map of India (Not to Scale) exhibiting marine transgression from eastern flank
 120 through Khemgaon, Sikkim and western flank through Narmada rift Source: (Chatterjee and
 121 Mathews et al. 2020).

122 A prominent sedimentary feature of the study area is the occurrence of coal-bearing heterolithic
 123 units, belonging to middle to upper Barakar formation. Heterolithic and tidally influenced
 124 depositional systems have been widely documented across various basins worldwide, reflecting
 125 diverse marginal marine to estuarine environments (Figure 2). Studies (Table 2) from formations
 126 such as the Ediacara Member in South Australia (Jenkins et al. 1983), the Tilje and Cook
 127 formations in offshore Norway (Martinius et al. 2001; Ringrose et al. 2005), the McMurray
 128 Formation in Canada (Gingras et al. 2016), Beach Formation in Australia (Bann et al. 2004),
 129 Ostreaelv Formation in East Greenland (Ahokas et al. 2014), Neslen Formation in Utah USA

130 (Olariu et al. 2015) and the Mamu and Nanka formations in Nigeria (Dim et al. 2019; Ogbe and
 131 Osokpor 2021), reveal the significance of tidal processes in shaping heterolithic successions.
 132 These interpretations are supported by sedimentological, ichnological, and stratigraphic evidence,
 133 emphasizing the role of transgressive-regressive events, fluvio-tidal interactions, and storm
 134 influences in the deposition of these units. (Table 2)



135
 136 **Figure 2:** Representative examples of heterolithic units deposited in tidal and fluvio-tidal
 137 environments across the globe. (Global shape file Source:
 138 <https://public.opendatasoft.com/explore/dataset/world-administrative-boundaries/export/>,
 139 accessed on 26/5/2025).

140 **Table 2:** Compilation of case studies on tidal/fluvio-tidal depositional environments, reported from
 141 various global locations. *-Coal reported alongside heterolithic unit.

Geological Description	Location	Paleo Depositional Environment	Reference
Ediacara Member of the Rawnsley Quartzite, context of Ediacara assemblage (Late Precambrian)	South Australia	Heterolithic siltstone/sandstone units represent intertidal deposits	(Jenkins et al. 1983)
Cook Formation; electrofacies analysis (Lower Jurassic)	Gullfaks Field, Offshore Norway *	Tide-dominated estuarine to deltaic setting	(Gupta and Johnson 2001)
Heterolithic unit, Tilje Formation (Early Jurassic)	Offshore mid-Norway	Tide-dominated	(Martinus et al. 2001)

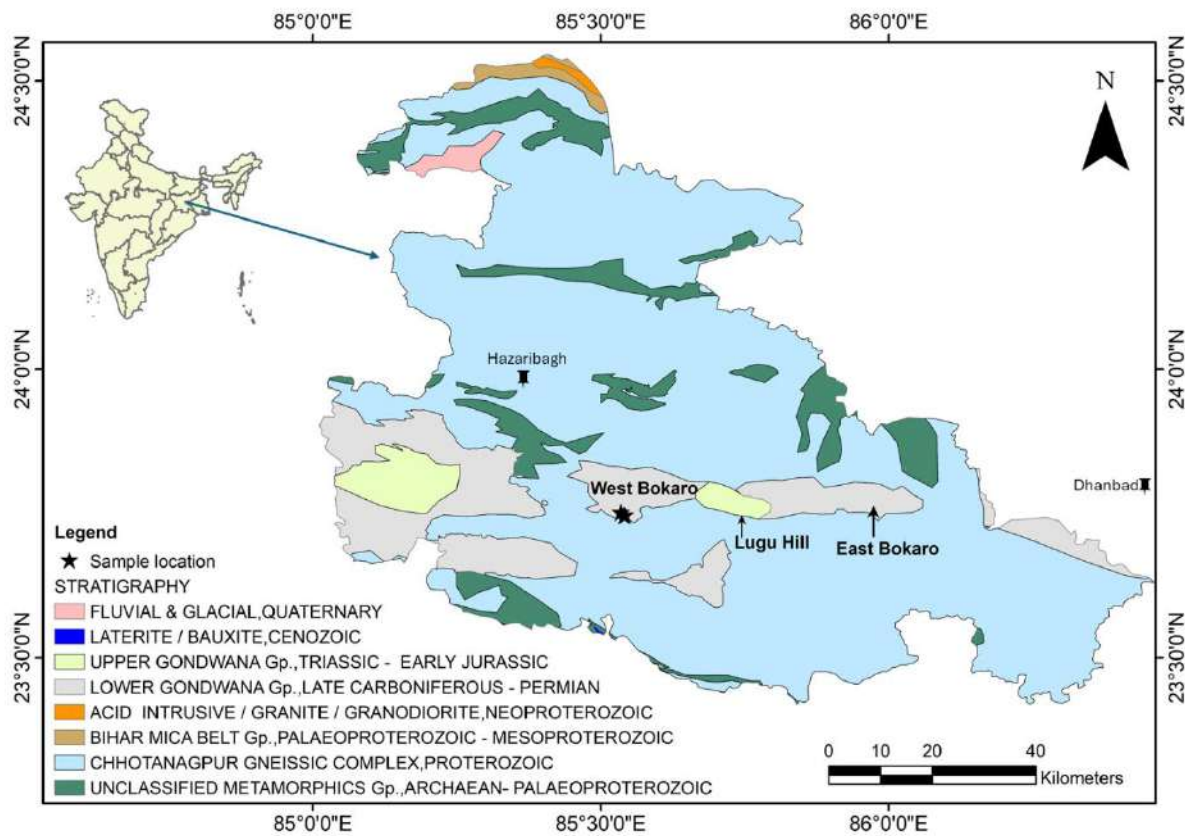
Pebbley Beach Formation; differentiation of estuarine vs offshore marine deposits using ichnology and sedimentology (Permian)	Sydney Basin, Australia	Brackish water to fully marine units	(Bann et al. 2004)
Heterolithic siliciclastic unit with diagenetically altered sandstones	Halten Terrace, mid-Norway *	tide-dominated deltaic and estuarine environments	(Martinius et al. 2005)
Vertical permeability estimation in heterolithic units, Tilje Formation	Offshore mid-Norway	Tidal deltaic sedimentary systems	(Ringrose et al. 2005)
Incised valley fills of Toarcian Ostreælv Formation; heterolithic succession	Jameson Land, East Greenland	Tide-dominated estuary	(Ahokas et al. 2014)
Campanian Neslen Formation; unusual fluvial-tidal channels with inclined heterolithic strata	Utah, USA *	Tidal influenced fluvial channels	(Olariu et al. 2015)
McMurray Formation; significance of cross-stratified sand, heterolithic unit, bioturbated channel sands.	Alberta, Canada	Bar-top / tidal-flat deposits	(Gingras et al. 2016)
Campano-Maastrichtian Mamu Formation; consists of carbonaceous shales, siltstones, sandstones, heteroliths and coal seams	Anambra Basin, Nigeria *	High frequency transgressive and regressive events in coastal swamps and lagoons, marginal marine environment	(Dim et al. 2019)
The ichnological variation in the heterolithic units, McMurray Formation;	Western Canadian Basin	Fluvio-tidal setting, marginal marine	(Melnyk and Gingras 2020)
Cyclical heterolithic layering, Lambir Formation (Middle Miocene)	Baram Delta Province, north-west Borneo	Fluvio-tidal setting, marginal marine	(Collins et al. 2020)
Nanka Formation of Ameki Group; depositional facies, sequence stratigraphy, reservoir potential (Eocene)	Southeast Nigeria	Tidal mudflat facies, marginal marine	(Ogbe and Osokpor 2021)

142

143 **2 Geology of the Study area**

144 The Bokaro basin is an E-W trending, linear, isolated depressions located in the eastern side of
 145 Indian Gondwana Basin Belt (Jha and Sinha 2022). The major basins of the West Damodar valley
 146 are typically synclinal half-basins, generally opening either to the west (such as Ramgarh, and
 147 Auranga-Hutar) or to the south (like North Karanpua). The notable exception is the narrow Bokaro

148 Basin, which is closed at both ends (Dutt 2019). The Lugu Hill, rising to ~978 m, is the dominant
 149 geomorphic feature that divides East Bokaro from West Bokaro (Murthy 2017) (Figure 3). West
 150 Bokaro basin is located in the Ramgarh district of Jharkhand, India (Sinha and Gupta 2020). The
 151 coalfield lies between 23°41' to 23°52' N latitude and 85°24' to 85°41' E longitude, covering an
 152 area of 207 sq km (Figure 3) (Tiwari et al. 2016b). We investigated the geological section exposed
 153 near Ara and Dumarbera villages in the Ramgarh district (Figure 4).

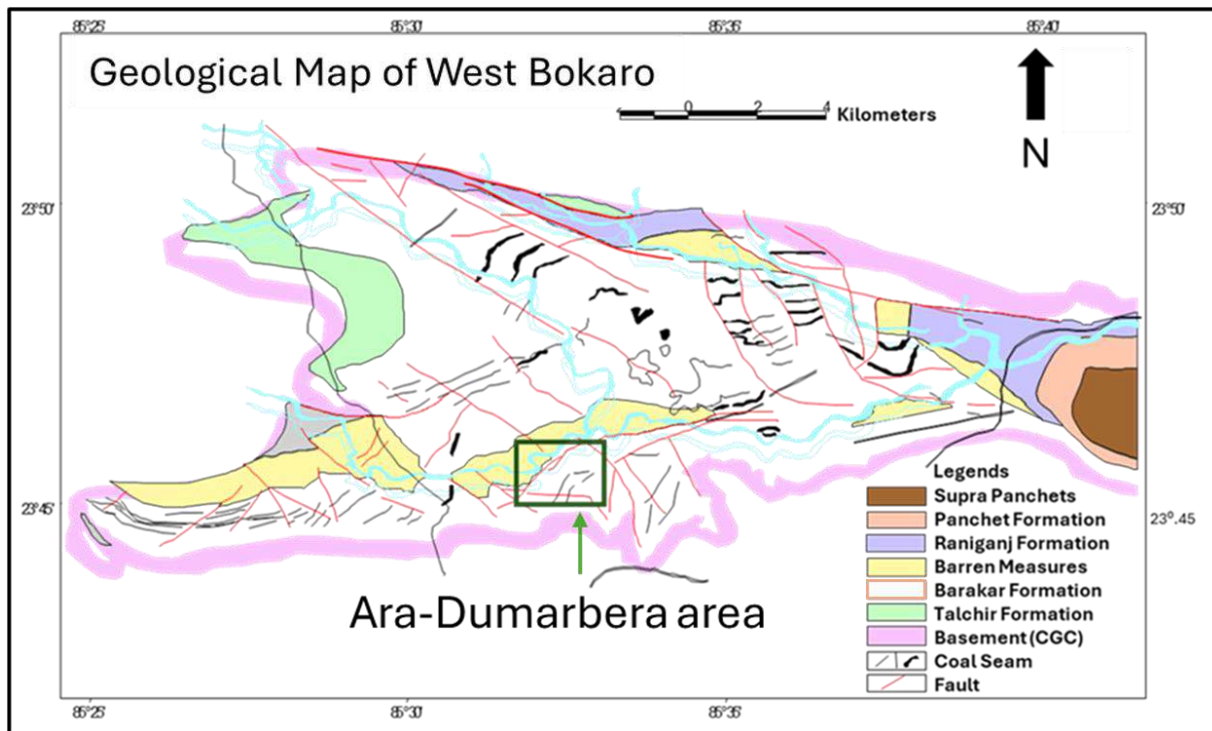


154

155 **Figure 3:** Location map of West Bokaro Basin along with the major stratigraphic unit exposed in
 156 the district of Hazaribagh, Ramgarh, and Bokaro, Jharkhand, India. Source: Bhukosh,
 157 www.bhukosh.gsi.gov.in (Accessed on 12-April-2025).

158 The West Bokaro coalfield is divided into two sub-basins by a twin synformal structure, with a
 159 northern and southern synform separated by an indistinct central antiform running in an east-west
 160 direction. The northern and southern sub-basins are separated by the Archean highland around
 161 Mandu (Tiwari et al. 2016b). These three structural axes converge in the eastern part of the
 162 coalfield. In the northern limb of the northern synform, the strata typically dip 15° to 25°

163 southward. In the southern limb of the northern synform, dips vary between 5° to 15° towards the
 164 north, except in the sub-basinal structures of the Tapin and Parej blocks. For the southern synform,
 165 the southern limb dips northward between 10° to 30° . The tectonic lineaments in these valleys
 166 have preserved the oldest rocks, which form the Archean basement complex, with the Permo-
 167 Carboniferous to Late Permian age Lower Gondwanan coal deposits overlying these basement
 168 rocks (Navale and Saxena 1989). To the North of the Bokaro basin, the Precambrian rocks are
 169 separated from the Gondwanas by a boundary fault while to the South and West the Gondwanas
 170 generally overlie the Precambrian with a profound unconformity (Raja Rao 1987).



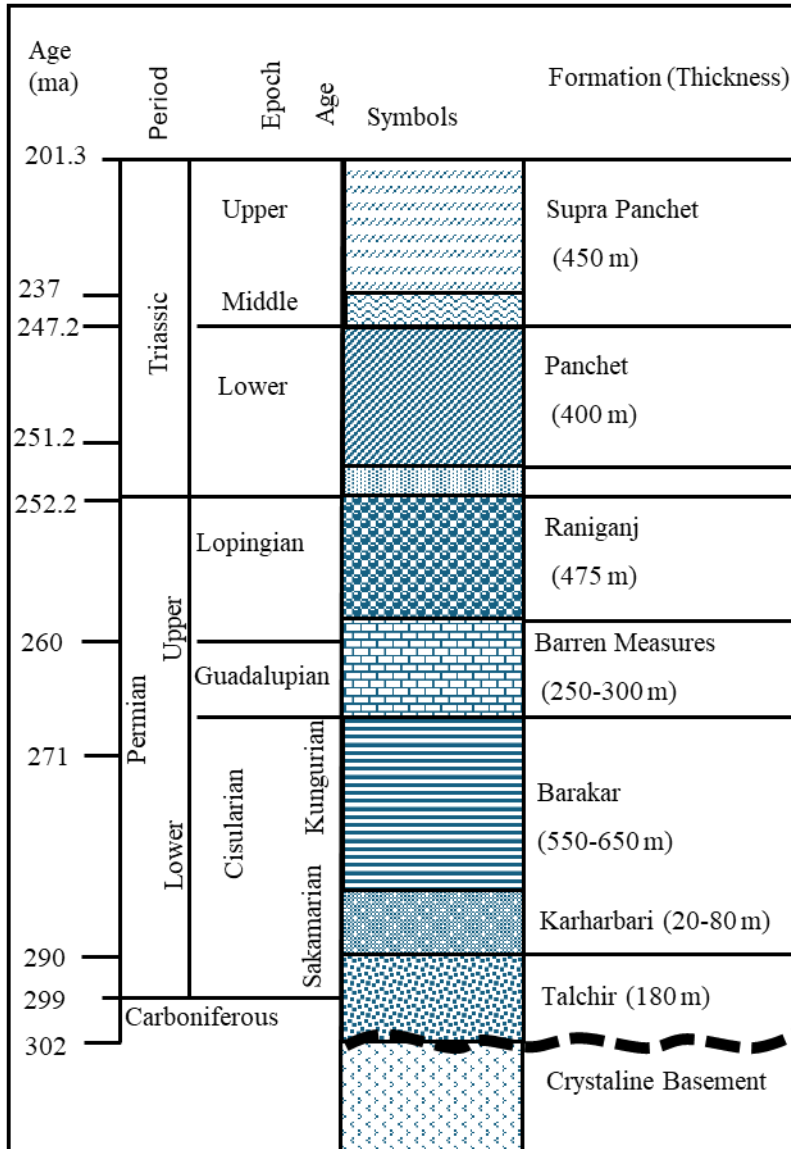
171
 172 **Figure 4:** Location map of West Bokaro Basin along with the major stratigraphic unit exposed in
 173 the West Bokaro, Jharkhand, India. Reproduced from (Srivastava et al. 2025).

174 2.1 Sedimentation and marine influence in the Bokaro Basin

175 The basin features a complete sequence of Lower Gondwana formations resting unconformably
 176 on the basement rocks (Tiwari et al. 2016a). It comprises formations including Talchir, Karharbari,
 177 Barakar, Barren Measures, Raniganj, Panchet, and Supra Panchet, spanning from the Early
 178 Permian to the Upper Triassic (Raja Rao 1987). Gondwana sedimentation begins with the Talchir
 179 Formation, which features glacial conglomerates, sandstone, and shales, resting directly on the

180 Precambrian basement rocks of amphibolite and granitoids, and is well exposed along Dudhi Nala
181 Mahato & Srivastava 2023). The Karharbari Formation, with limited exposure in this region,
182 consists of sandstones, shales, and thin coal seams.

183 The Barakar Formation (Early Permian) of the Lower Gondwana succession is the predominant
184 coal-bearing litho-unit of the West Bokaro Basin, similar to the rest of the peninsular Indian coal
185 fields. This formation typically features thick coal seam-bearing sedimentary sequences in this
186 region (Bhattacharya and Banerjee 2015; Bhattacharjee et al. 2018). Dominating the area, the
187 Barakar Formation covers a major part of the coalfield and has an aerial extent of $\sim 125 \text{ km}^2$. It
188 comprises of coarse to fine-grained sandstones, pebbly conglomerates, gritty sandstones, gray
189 shales, carbonaceous shales, fireclays, and coal seams (Tiwari et al. 2016b). The study area is
190 primarily characterized by the cyclic sequence of Barakar formation, consisting of sandstone of
191 various grain size, carbonaceous and grey shales and coal seams. The full sequence of Barakar
192 Formation in West Bokaro basin contains 14 regionally correlatable coal seams. The Barren
193 Measures Formation is mainly composed of sandstone and shale, while the Raniganj Formation,
194 which overlies the Barren Measures, marks the end of the Lower Gondwana sedimentary sequence.
195 Due to the synclinal structure of this coalfield, which extends in an east-west direction, the Barakar
196 Formation is exposed on both the northern and southern limbs of the syncline, while the younger
197 Barren Measures and Raniganj Formations occupy the central axial region (Sinha and Gupta 2020)
198 (Figure 4). Figure 5 provides the generalized stratigraphic successions of the West Bokaro Basin.



199
200 **Figure 5:** Generalized stratigraphic succession of West Bokaro basin modified after (Murthy
201 2017).

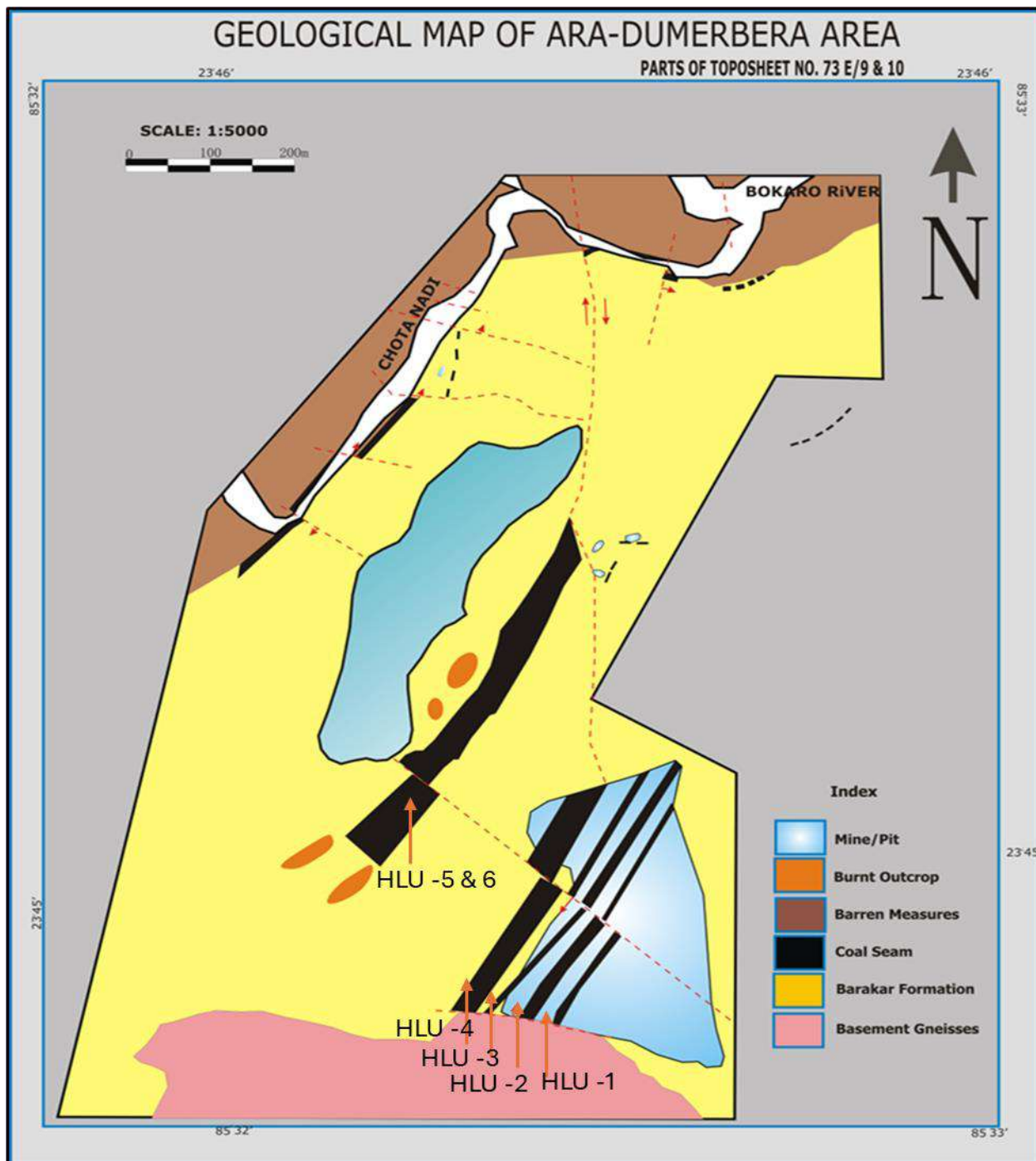
202 **3 Methodology**

203 Researchers use fossil records, pollen and spores, sedimentological records, geochemical
204 composition and several other tools and techniques to interpret paleo-depositional environments
205 (Spiro et al. 2019). Biological entities, sensitive to environmental changes, provide precise
206 paleoenvironmental information, but their absence in some sediments can hinder predictions.
207 Geochemical entities, while often present, can undergo post-genetic alterations, leading to
208 potential inaccuracies. Therefore, integrating multiple methods offers a comprehensive

209 understanding of the paleo depositional environment, with each technique complementing the
210 others. Hence a holistic multi proxy analysis was considered for the identification of traces of
211 marine transgression, in this region, at the time of sedimentation of the Barakar Formation.

212 **3.1 Field Study: Sedimentology**

213 Fieldwork covered areas along the Chhota Nadi River and coal mining pits near the villages of Ara
214 and Dumerbera, close to Kuju town in Ramgarh District, Jharkhand, India. The area mapped by
215 two of the authors SKB and MKS at the scale of 1:5000 (Figure 6) aiming at the following: (i)
216 Identification of lithological characteristics and their lateral and vertical continuity, as well as the
217 contact relationships with underlying and overlying sequences. (ii) Role of the faults in the
218 disposition of the strata. (iii) Understanding changes in lithological features, such as grain size.
219 This can help to determine whether the sequence is coarsening or fining upward, which can then
220 be interpreted within the context of marine transgression-regression cycles. (iv) Identification of
221 sedimentary and biogenic structures, which can provide essential clues for determining the
222 sedimentary depositional environment. Coal seams are only exposed in the nala section and
223 abandoned quarry. Accordingly, it has been marked in the map.



229 samples (Heterolithic Unite (HLU) 1=7, HLU 3=15, HLU 5=15, HLU 6=17), 6 shale samples, and
230 4 sandstone samples were collected (Figure 7). During macroscopic examination, consecutive coal
231 samples with similar characteristics were combined to reduce the sample count. Consequently, the
232 number of coal samples was reduced to 24 (HLU 1=5, HLU 3=6, HLU 5=6, HLU 6=7), and the
233 number of shale samples was reduced to four.

234 The coal samples were broken into smaller pieces and air-dried at room temperature in the
235 laboratory. Once dried, the samples were crushed with a mortar and pestle, then sieved to achieve
236 two mesh sizes: < 18 and < 72 mesh. A portion of the < 72 mesh samples was further ground to <
237 100 mesh using a Vibratory cup mill (HVC-2.065).

238 The samples were analyzed for minerals, major oxides, and trace elements using X-ray
239 Fluorescence Spectroscopy (XRF). For XRF, press pellets were prepared from <100 mesh
240 powdered coal, utilizing the natural moisture present in the coal and shale as a binding agent. XRF
241 was conducted on Malvern Panalytical XRF Spectrometer at the Geology and Geochemistry
242 laboratory, Rajiv Gandhi Institute of Petroleum Technology (RGIPT), Jais, India. This method
243 identified major oxides and trace elements in coal and shale samples.

244 **3.3 Micro-petrography:**

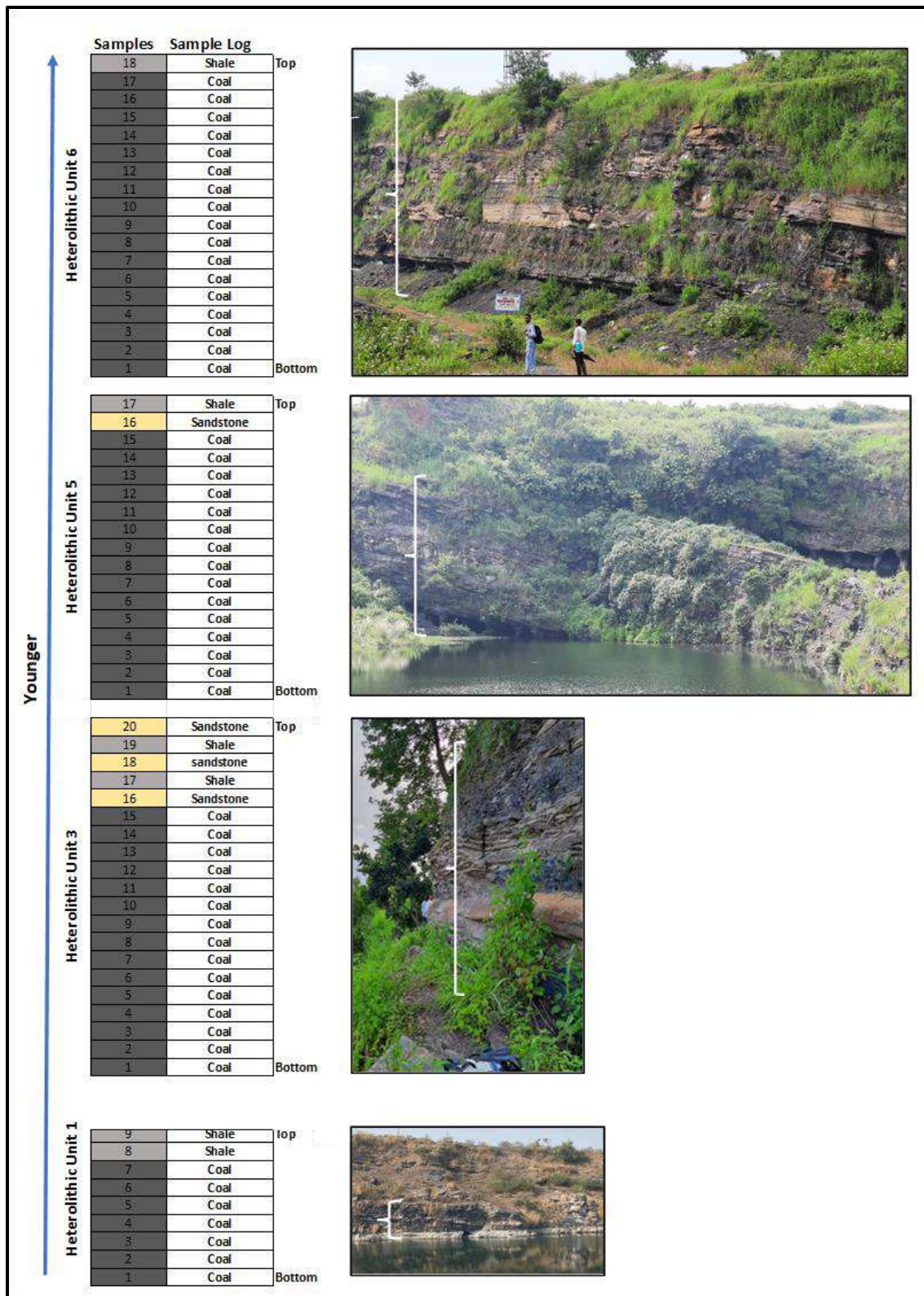
245 For micropetrography, the coal and shale samples were crushed and sieved to a size of < 18 mesh.
246 Particulate pellets were then prepared from these samples using cold-setting material without
247 applying pressure. The sample pellets were polished and examined using an advanced petrological
248 microscope (Leica DMP2700P) equipped with LASv4.6 analysis software and an imaging system.
249 Immersion oil (refractive index of 1.518 at 23 °C) served as the medium between the microscope
250 objective and the sample. The petrography followed the ICCP Classification (ICCP, 1998, 2001;
251 Pickel et al., 2017) and ISO standard (ISO:7404-5, 2004). This analysis provided valuable insights
252 into the mineralogic and maceral composition of coal and shale samples.

253 **3.4 Scanning Electron Microscopy with Energy-Dispersive X-ray Spectroscopy (SEM-EDX) 254 Analysis:**

255 The minerals in coal samples were examined through SEM-EDX. A chip of ~ 1 cm in size was
256 extracted from coal sample, coated with gold, and analyzed using the SEM JEOL (Make), JSM-
257 7900F (Model) in an airlock chamber at the Central Instrumentation Facility (CIF), RGIPT, Jais,

258 India. The analysis identified various mineral types. Several line scans were performed on the
259 sample to obtain insights into its elemental composition, facilitating the identification of minerals
260 within the coal samples.

261



262

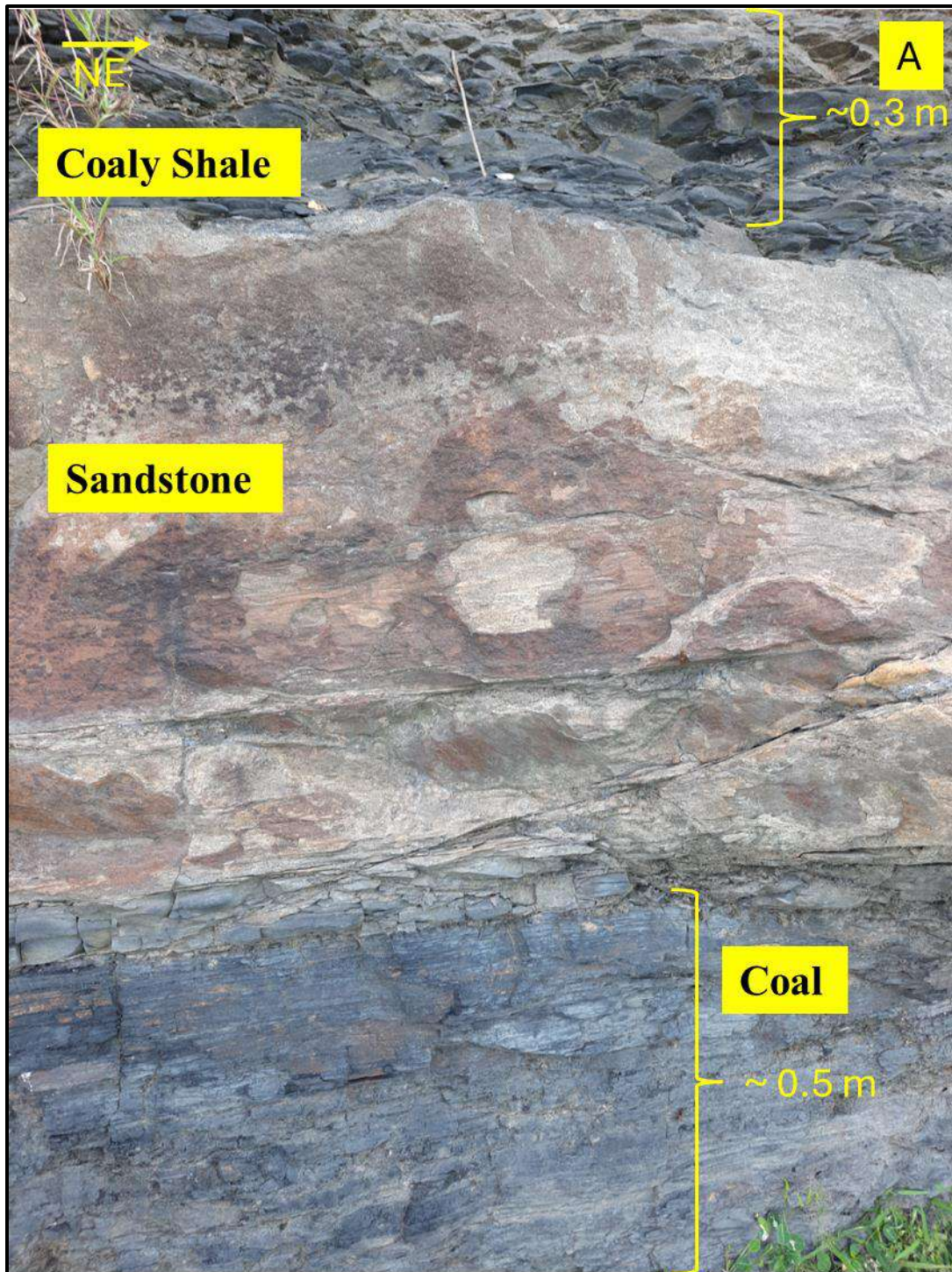
263 **Figure 7:** Sampling profile of four heterolithic units (younger at top), and their corresponding field
 264 photographs.

265 **4 Results & Discussions**266 **4.1 Field Evidence**

267 The lithologic, bioturbation, and sedimentary structural characteristics were examined and
268 recorded during the geological field work around Ara Mine, Kuju area. The geological succession
269 is represented by ~ 610 m-thick sedimentary sequence of Barakar Formation. The following
270 sedimentary facies, belonging to upper part of Barakar Formation have been identified in the
271 studied area- (i) coal and coaly shale unit, (ii) splintery black shale facies; (iii) wavy and flaser
272 bedded heterolithic facies (iv) sandstone with wave ripple laminated facies; (v) hummocky cross
273 stratified fine grained sandstone facies; (vi) trough cross stratified sandstone facies; and (vii)
274 epsilon cross-bedded sandstone facies. These facies are described below.

275 **4.1.1 Coal and coaly shale facies:** These facies are always present at the bottom of the heterolithic
276 unit (Figure 8 A). The coal seam is 1-3 m thick. The coal typically appears dark and somewhat
277 glossy, with a moderate specific gravity. It exhibits interlayer bands of vitrain-clarain and vitrain-
278 durain, with negligible amounts of fusain present. These coals mostly lie in the macro lithotype
279 category of banded to banded bright as per Diesel's classification (Figure 8 B).

280 Interpretation: The formation of these thick coal seams likely resulted from the accumulation of
281 plant material and minor terrigenous sediments in a marsh environment (Scott 1987). Extensive
282 coal layers developed in low-lying peat mires, where limited siliciclastic input allowed for the
283 prolonged accumulation of vegetation. The brightness of these coals, attributed to the abundance
284 of vitrain, reflects a high vitrinite content. This suggests that the peat swamps had excellent
285 preservation conditions, with a consistently high-water table keeping the organic matter submerged
286 and well-preserved. Periodic influxes of siliciclastic buried the organic material, eventually
287 transforming it into coal. The presence of these facies alongside tidal-flat deposits indicates that
288 the environment was plausibly a supratidal marsh.





290

291 **Figure8:** Vertical sections. **A.** Coal and coaly shale facies, and **B** banded to banded bright coal,
 292 exposed near Ara-Dumarbera village, Kuju, Ramgarh, India.

293 **4.1.2 Splintery black shale facies:** Black coloured carbonaceous shale, 0.5-1 m thick, splintery
 294 in nature. Parallel laminated, along the bedding plane an array of plant leaves is well preserved.
 295 Sometimes, thin coal units (10-20 cm thick) are present in between these lithofacies (Figure 9).

296 Interpretation: Deposited due to suspension fall out under stagnant calm water for quite a longer
 297 period. However, under deeper water conditions where anoxic conditions exist having input of
 298 plant debris (Schieber 1989; Arthur and Sageman 1994).



301 **Figure 9:** Vertical sections. A. Splintery black shale facies (viewing towards NNW) and B.
 302 Zoomed view of Splintery black shale facies, starting from the base of the pen, Part of HLU-3,
 303 exposed near Ara-Dumarbera village, Kuju, Ramgarh, India. (The length of the pen is 14 cm)

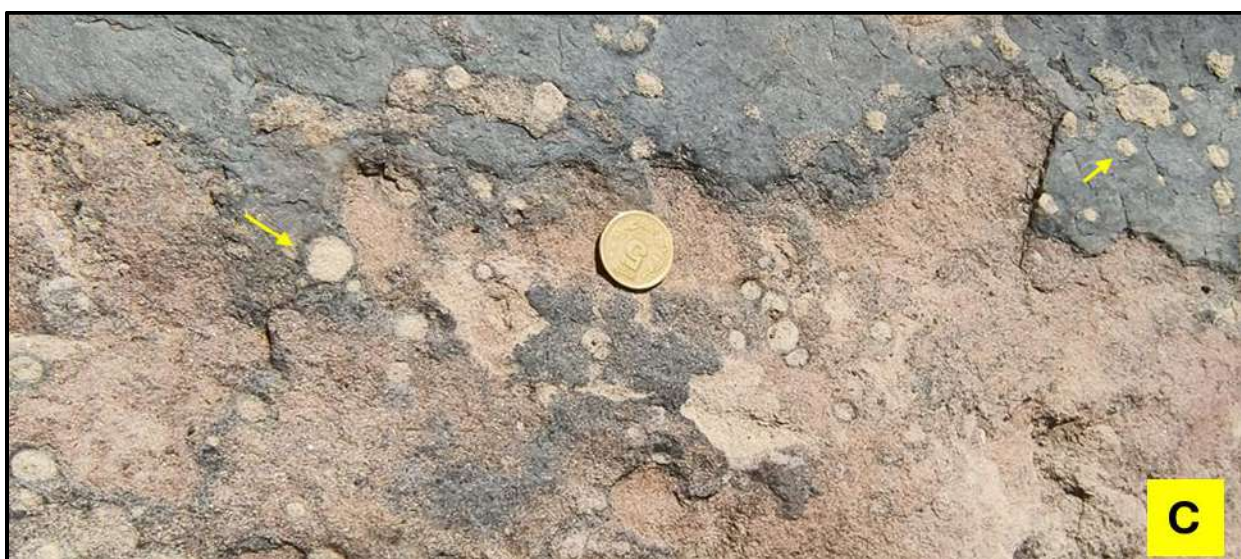
304 **4.1.3 Wavy and flaser bedded heterolithic facies:** At least 6 to 7 heteroliths were present in this
 305 area. Black to dark grey, 10 to 50 cm thick mudstones with thin siltstones and high concentration
 306 of plant debris. Falser and wavy bedded mm to cm thick sandstone–mudstone beds and lamination
 307 (Figure 10 A), shows systematic changeover between different beddings, present as heterolithic
 308 units of 10-20 cm thick. Cyclic sequence of coal, siltstone/black shale, siltstone-sandstone
 309 rythmites, and sandstone is commonly present within the heterolithic units. Fine to very fine

310 grained bioturbated sandstone-mudstone heterolith with variety of ichnofossils having thickness
311 of 20-60cm (Figure 10 B and C).

312 Interpretation: Characteristically formed in intertidal areas by alternate traction load and
313 suspension load deposition (Reineck and Singh 1980). The cyclic sequence represents a tidal
314 bundle characterized by a fluctuating coarsening-upward trend, formed as a result of marine
315 transgression. Fine to very fine grained bioturbated sandstone-mudstone heterolith deposited under
316 low energy calm condition with sub-aerial exposure.



317



320 **Figure 10: A.** Wavy and flaser bedded heterolithic facies, facing towards NNW, **B.** Plan view,
321 Bioturbated fine-grained sandstone and mudstone with *Diplocriterion*, and **C.** *Skolithos isp.*

322 ichnofossils from part of HLU-3, Barakar Formation, Dumerbera Village, District: Ramgarh,
 323 India.

324 **4.1.4 Sandstone with wave ripple laminated facies:** These facies are characterized by fine-to-
 325 medium grained relatively well sorted sandstone with symmetrical oscillation ripples. Bundle up-
 326 building and mud-drapes are common features of these facies (Figure 11). At places, this unit also
 327 occurs as a part of the heterolithic facies.

328 Interpretation: Symmetrical ripples i.e. wave ripples formed by the oscillation of shallow waves
 329 with intermittent aerial exposures in an open shore environment (Reineck and Singh 1980).



330
 331 **Figure 11:** Wave generated cross laminations, HLU-5 (demarcated by yellow arrow, facing
 332 towards N), Dumarbera village, Kuju, District: Ramgarh, India.

333 **4.1.5 Hummocky cross-stratified fine-grained sandstone facies:** These facies are comprised of
334 moderate to well-sorted, fine-grained, buff, and light to dark pink color sandstone beds of couple
335 of meters in thickness and of less lateral extension. The total thickness of these facies varies from
336 0.5 to 1 m and have discontinuous mud drapes. Mica flakes, mainly muscovite, is one of the
337 dominant constituents of sandstone. Small scale wave ripples are also associated with these facies
338 and are dominant at the upper part of these facies. In the Lower part, below Dumerbera Sandstone
339 a Hummocks and Swales are preserved having ~ 1.5 m trough length (Figure 12 A, B).

340 Interpretation: Deposition might have taken place under storm generated oscillatory flows below
341 fair-weather wave base i.e. mainly at sub-tidal zone of shoreface. The presence of mica flakes
342 indicates deposition mainly under calm and quite condition where settling is dominated with an
343 impulsive storm wave effect.



344



345

346 **Figure 12: A.** Hummocky cross stratified sandstone, (HLU-3), facing towards NNW. **B.** Zoomed
 347 view of hummocky cross-stratified sandstone, facing towards N (HLU-5), Barakar Formation,
 348 (paleocurrent direction demarcated by yellow arrow), Kuju, District: Ramgarh, India.

349 **4.1.6 Trough cross stratified sandstone facies:** It is a coarse-grained, medium to poorly sorted,
 350 feldspathic sandstone, 1-2 m thick beds with scoured lower bounding surfaces having pebbles and
 351 conglomerate at the base. Two large-scale trough cross stratified sandstone beds were identified in
 352 the study area. The Dumarbera sandstone displays the characteristics of these facies and is exposed

353 extensively in this area (Figure 13). The upper sandstone litho-unit is known as Parsatoli sandstone,
 354 which overlies the heterolithic unit.

355 Interpretation: It might be produced by the downstream migration of 3-D sub-aqueous dunes under
 356 relatively high flow regime (Leclair 2002). Scoured base has been formed because of erosion by
 357 the huge bed load under a high energy condition.



358

359 **Figure13:** Large-scale trough cross-bedded sandstone lithofacies showing unidirectional
 360 palaeocurrent (demarcated by red arrow), Dumarbera Sandstone bed; Near Dumarbera village, Kuju,
 361 District: Ramgarh, India. (Facing towards ESE)

362 **4.1.7 Epsilon cross-bedded sandstone facies:** These facies are mainly observed in the Chota Nadi
 363 Section at the top of upper Barakar i.e. Parsatoli Sandstone. This is characterized by the large-scale
 364 trough cross stratified, multi-storied, coarse to very coarse-grained sandstone with lateral accretion
 365 surfaces. (Figure 14).

366 Interpretation: Lateral accretion surfaces formed as a product of the migration of point bar deposit
 367 under meandering channel (Willis and Tang 2010).



368

369 **Figure 14:** Epsilon crossbedding, present in Parsatoli sandstone beds, topmost part of the Barakar
 370 Formation, located on the right bank of the Chhota Nadi. (Facing towards N)

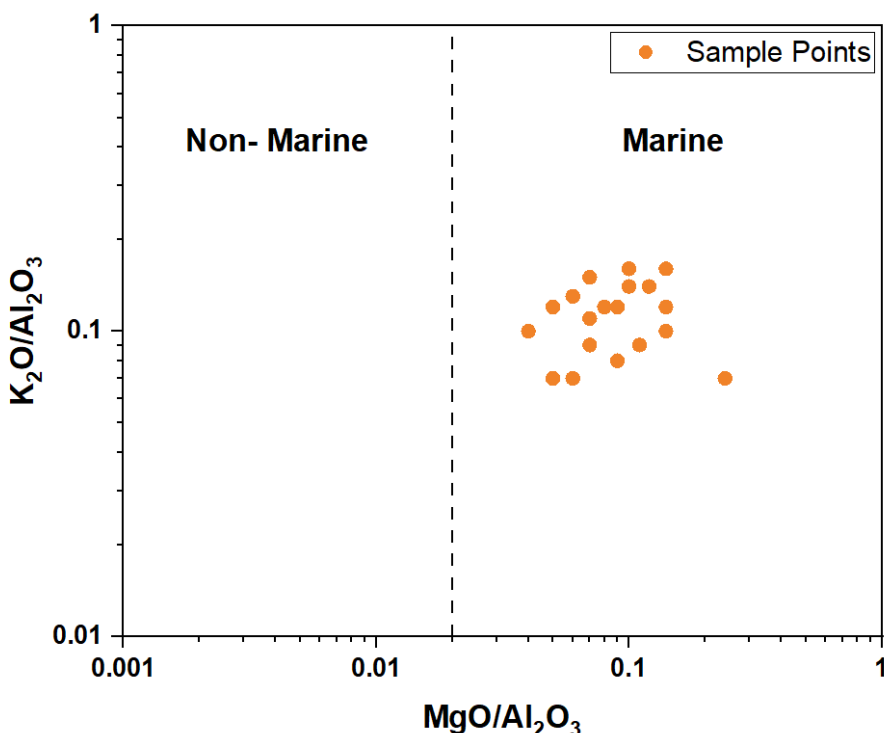
371 **4.2 Geochemical evidence:**

372 The presence and distribution of specific clay minerals, major oxides and trace elements are
 373 influenced by the depositional environment. As a result, their compositions and ratios can serve as
 374 indicators to reconstruct ancient depositional settings (Srivastava et al. 2024). A multiproxy
 375 approach has been chosen for the reconstruction of paleo depositional, as no specific proxy is
 376 robust enough to be used individually (Wei and Algeo 2020).

377 **4.2.1 Major element geochemistry:** Vassilev et al. (2010) documented in detail that certain oxide
 378 ratios have been employed in the literature as geochemical markers for coal formation, based on
 379 geochemical data derived from coal originating from diverse geologic settings (Vassilev et al.
 380 2010). For instance, coal with low ratios of $\text{CaO} + \text{MgO}/\text{K}_2\text{O} + \text{Na}_2\text{O}$ and CaO/MgO indicates
 381 deposits influenced by marine or brackish conditions, saline lakes, or organic matter rich in algal
 382 remains (Ameh 2019; Vassilev et al. 2010). Elevated Mg concentrations in certain minerals are
 383 characteristic of coal beds affected by marine transgressions (Stach et al. 1982). Vassilev et al.
 384 (2010) reported that CaO/MgO ratios between 0.9 and 1.4 were found in coals influenced by
 385 marine or brackish water or enriched in algal remains, while coals with higher ratios were of non-
 386 marine origin (Vassilev et al. 2010).

387 In the studied coal samples, the value of Ca and Mg ranges up to 0.92 % (mean 0.39%) and 0.10
 388 % to 0.53 % (mean 0.23%) respectively, whereas the CaO/MgO ratio ranges from 0 to 3.44 (mean
 389 1.51). These values suggest that the coal seams may have experienced episodic marine / brackish
 390 water influence during peat accumulation or might have got contributions from algal remains.

391 The MgO/Al₂O₃ ratio also serves as an effective geochemical indicator for distinguishing marine
 392 from non-marine influences. MgO is typically more abundant in marine deposits, whereas Al₂O₃
 393 is characteristic of continental weathered debris, often resulting from the breakdown of feldspar.
 394 The relationship between log(K₂O/Al₂O₃) and log (MgO/Al₂O₃) can be utilized to distinguish
 395 marine sediments from non-marine ones (Bhattacharjee et al. 2018). The studied samples plotted
 396 on the aforementioned graph clearly indicate that sediments were deposited in a marine
 397 environment (Figure 15).



398
 399 **Figure 15:** Log-Log Cross-plot between (MgO/Al₂O₃) and (K₂O/Al₂O₃) (as in Bhattacharjee et al.
 400 2017) depicts the depositional environment of all the studied samples.

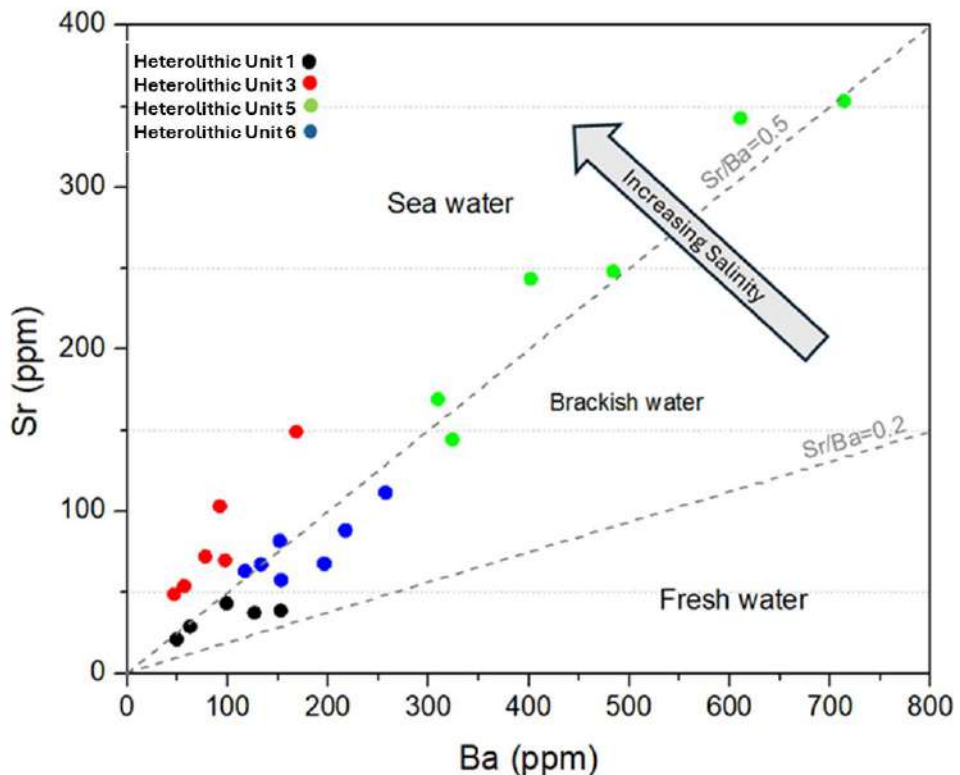
401 **4.2.2 Trace element geochemistry:** Strontium (Sr) and barium (Ba) are reactive alkaline earth
 402 metals frequently found on Earth as either sulfates (SrSO₄ and BaSO₄) or carbonates (SrCO₃ and

403 BaCO_3). In seawater, barium can appear as Ba^{2+} ions, BaSO_4 (barite), or as particulates in
404 sediments. The concentrations of Sr and Ba are influenced by seawater chemistry and geological
405 settings. Sr is more soluble in seawater compared to Ba and has a higher solubility product.
406 Barium's concentration remains relatively stable in seawater due to lateral circulation, except in
407 regions of upwelling or significant freshwater input (such as at large river mouths). Increased
408 salinity promotes the precipitation of Sr over Ba, thereby elevating the Sr/Ba ratio (Zuo et al.
409 2020). Therefore, the Sr/Ba ratio serves as a geochemical marker for estimating paleo salinity
410 levels. A ratio > 1 indicates seawater, between 1 and 0.6 suggests brackish water, and < 0.6
411 connotes freshwater (Li et al. 2018) . Concentration of Sr and Ba ranges from 0.02 % to 0.35 %
412 (mean 0.12 %) and 0.05 % to 0.71 % (mean 0.23 %) respectively. The Sr/Ba ratio of the studied
413 samples (0.25-1.12, mean of 0.6) suggests that the Barakar Formation experienced a variable
414 depositional environment influenced by seawater, brackish water and freshwater inputs.

415 In another exercise, the concentrations of Sr and Ba (in ppm) marked on a Sr-Ba cross-plot, shows
416 that the data points are dispersed within the marine facies to brackish water facies (Figure 16). The
417 data in the plot depicts that heterolithic unit 3 was deposited entirely under seawater inundation,
418 whereas heterolithic units 1, 5, and 6 were deposited in a transitional zone environment with lower
419 salinity. This distribution indicates that the Early Permian coals of the Barakar Formation were
420 predominantly deposited under the influence of marine transgression-regression cycle.

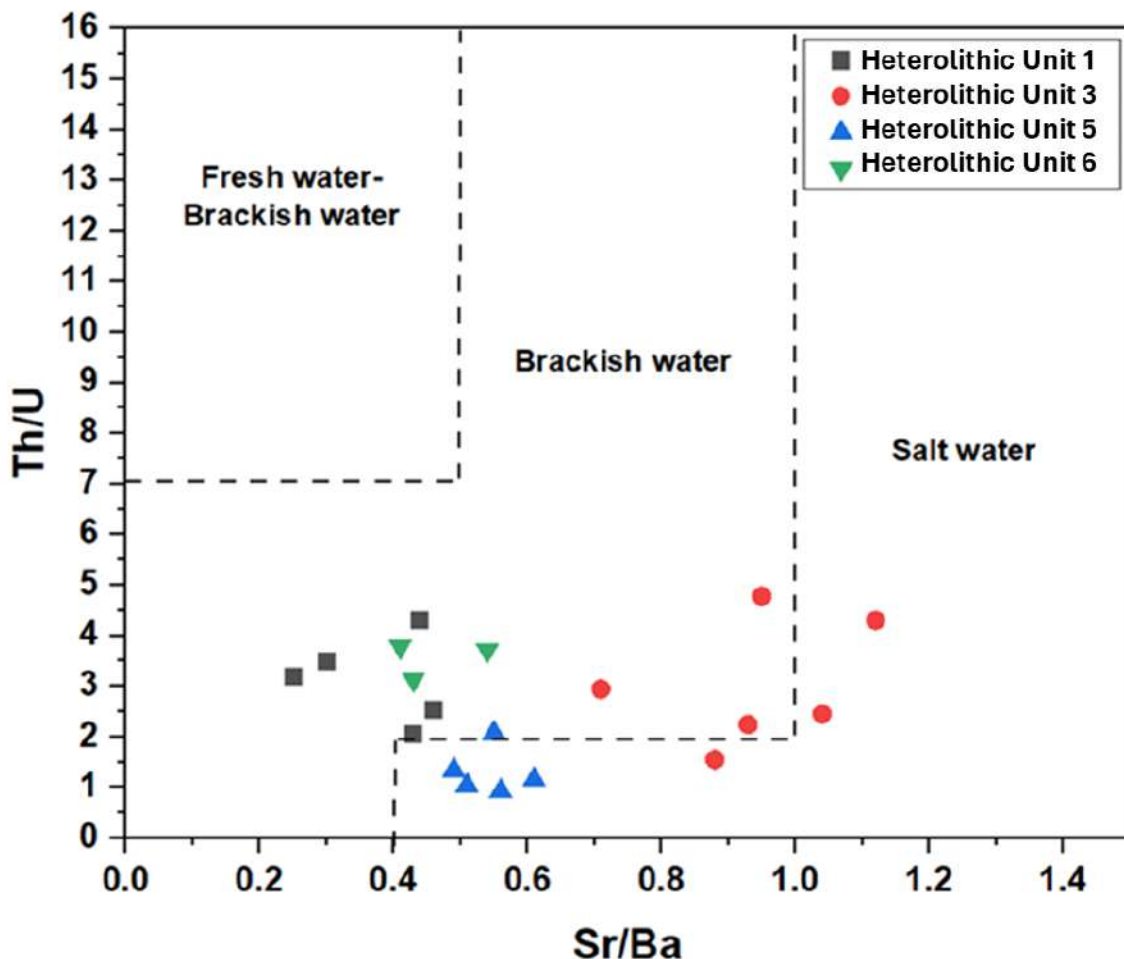
421 The Th/U ratio is often used as a geochemical proxy to infer paleoenvironmental conditions,
422 including paleo-salinity, though it provides an indirect determination. This ratio is particularly
423 valuable in sedimentary geology for assessing paleo-redox conditions. Typically, reducing
424 conditions are associated with freshwater or low salinity, while oxidizing conditions are linked to
425 marine environments. Thorium (Th) is relatively immobile in low-temperature surface
426 environments and remains in a constant oxidation state (Wei et al. 2023), whereas Uranium (U) is
427 more mobile and can exist in multiple oxidation states (Cumberland et al. 2016). In reducing
428 (anoxic) environments, U is often reduced to U^{4+} and precipitates out of solution, resulting in
429 higher Th/U ratios. Conversely, under oxidizing conditions, U remains as U^{6+} and is more soluble
430 (Borch et al. 2010), leading to lower Th/U ratios. Thus, a high Th/U ratio indicates reducing or
431 freshwater geological settings, while a low Th/U ratio indicates oxidizing or marine conditions.
432 Typically, a Th/U ratio > 7 suggests a terrestrial freshwater environment, a ratio between 2-7

433 indicates a brackish water environment, and a ratio < 2 points to a marine/saline environment (Fu
 434 et al. 2018). The Th/U ratio of the studied samples ranged from 0.93 to 4.78 (mean 2.53), indicating
 435 a brackish to saline water condition was prevailing at the time of deposition of the Barakar
 436 Formation.



437
 438 **Figure 16:** Plot of concentrations of Sr and Ba (Cao et al. 2022). show salinity in the coal samples
 439 collected from different heterolithic units in the study area.

440 In another cross-plot analysis between Th/U and Sr/Ba, a similar interpretation can be drawn:
 441 heterolithic unit 3 falls entirely within the seawater region, whereas heterolithic units 1, 5, and 6
 442 fall between the seawater and brackish water regions. This supports the notion of a fluctuating
 443 depositional environment with frequent seawater inundation (Figure 17).



444

445 **Figure 17:** Cross-plot between (Th/U) and (Sr/Ba) (Pillai et al. 2023) depicting the depositional
 446 environment of the samples studied.

447 4.3 Mineralogical Evidence:

448 Carbonates are characteristic authigenic minerals in these coals, as evident from reflected light
 449 petrography (Figure 19 A-F). They most often either embed macerals, particularly collotelinite, or
 450 appear as crack-filling material in collotelinite or chamber-filling material in fusinite. The
 451 occurrence patterns of authigenic carbonates in coal sometimes indicate multiple phases of
 452 formation, spanning major syngenetic and epigenetic stages (Vassilev and Vassileva 1996). As
 453 observed during reflected light petrography, siderites are mostly present either as independent
 454 concretions (Figure 19 F) or show growth over collotelinites, whereas dolomites mostly embed
 455 collotelinite, reflecting a precipitation structure covering collotelinite or other macerals. The

456 calcites are mostly present as crack-filling or chamber-filling material. Observation from the
457 samples studied indicates that siderite and dolomite are syngenetic types, consistent with their
458 recognized global occurrence in coal deposits (Taylor et al. 1998).

459 **4.3.1 Dolomite:** The SEM-EDX analysis of coal samples from the study area reveals the presence
460 of various minerals and macerals. Line scans across several mineral assemblage groups indicate
461 the presence of minerals such as clay, silicates, and most notably, carbonates (Sample S3/B4). In
462 some areas, calcite was identified, and nearby, dolomite was also detected (Figure 18).
463 Additionally, the XRF analysis shows a high magnesium content in most samples, with
464 exceptionally high levels observed in a few specific samples. The high Ca and Mg levels are linked
465 to various causes including (1) formation of Mg-rich carbonates and sulfates; (2) Mg bound to
466 organic matter; (3) biogenic sources e.g., plants and fossils; (4) weathering of sulfides and
467 precipitation from water; and (5) detrital minerals e.g., montmorillonite, chlorite, and authigenic
468 minerals like brucite(Vassilev et al. 2010).

469 However, in this case the elevated levels of Mg are mostly attributable to the deposition of
470 syngenetic Mg-rich carbonate (dolomite). Source of Mg^{+2} that transforms calcite to dolomite
471 comes from marine or diagenetic environments. The dolomites in this case appear mostly in the
472 form of independent micro nodules or embedded coal particles. The possibility of diagenetic
473 alteration of calcite is less probable as no signs of active hydrothermal fluid were found by the
474 elemental geochemical analysis ($Al/(Al+Fe+Mn) > 0.4$ and $(Fe+Mn)/Ti < 15$). The elevated
475 concentration of magnesium indicates a saline environment, often associated with saline lakes or
476 coal deposits influenced by marine transgressions (Vassilev et al. 2010). Marine influence in the
477 dolomitization of coastal peat swamps occurs when magnesium-rich seawater infiltrates the
478 swamp environment during high tides, storm surges, or sea-level changes. This introduces
479 magnesium into the peat swamp, transforming calcium carbonate (from shell debris or plant
480 material) into dolomite. The interaction between marine waters and organic-rich sediments can
481 create conditions favorable for dolomitization, especially in areas where saline and freshwater mix,
482 altering the geochemistry of the swamp and influencing mineral deposition.

483 **4.3.2 Siderite:** Siderite was identified in only a few samples (S5/B3, S5/B4) (Figure 20) during
484 micropetrography, but where present, it appeared in abundance. It is commonly observed forming

485 on collotelinite grains or nucleating around other macerals, with typical radiating structure or
486 concretions embedded on a maceral (Figure 20).

487 Sideritization refers to the formation of the mineral siderite (FeCO_3) through the interaction of iron
488 with dissolved CO_2 , which is often produced by the decomposition of organic material. This
489 mineralization typically occurs in reducing settings with low sulfur content, such as coal seams or
490 organic-rich sediments. It is particularly characteristic of coal deposits formed in freshwater
491 environments, where sulphate-rich seawater and sulfide ions are absent, and under conditions that
492 promote strong reduction (Vassilev et al. 2010). However, the presence of siderite in modern salt
493 marshes, such as one present in Norfolk, UK, (Pye 1984; Pye et al. 1990) indicates that the
494 precipitation of siderite is more complex than previously assumed and might get affected by the
495 microbial activity (Lin et al. 2020a).

496 Siderite can only form in specific environmental conditions. It needs an oxygen-free (anoxic)
497 environment because dissolved iron (Fe^{2+}) reacts with carbonate ions (CO_3^{2-}) to create siderite, but
498 iron quickly oxidizes in the presence of oxygen. Additionally, hydrogen sulfide prevents siderite
499 formation by reacting with dissolved iron to form other minerals (Lin et al. 2020a).

500 For siderite to form, pH must be between 6.0 and 7.2; lower pH delays carbonate precipitation,
501 while higher pH favors the formation of other minerals like calcite. The process usually involves
502 microbial activity that generates dissolved iron and alkalinity, but just having bacteria that reduces
503 iron often raises the pH too high for siderites to form. So, additional conditions are needed for the
504 siderites to develop (Lin et al. 2020a). Siderite can form in the environments where iron reduction
505 takes place faster than sulfate reduction, resulting in an insufficient amount of dissolved sulfide to
506 bind with all the available ferrous iron in the solution (Pye et al. 1990). Thus, based on comparisons
507 with modern sedimentary environments, such as intertidal marsh and sandflat sediments of
508 Norfolk, England (Pye et al. 1990; Lin et al. 2020b;), it is likely that these siderites also formed in
509 an intertidal setting.

510 **4.3.3 Pyrite:** Fe sulfides are typical authigenic minerals in many coals (Vassilev and Vassileva
511 1996). However, in the currently studied samples, pyrite is relatively scarce (S3/B1 and S6/B5).
512 Despite its low abundance, it appears in various forms, most commonly as isolated crystals
513 dispersed within collotelinite macerals or, on several occasions, as encrustations in the cell lumens
514 of fusinite, where mineral deposits are preserved in the plant cell structure. In rare cases, pyrite is

515 also observed filling cracks within collotelinite (Figure 21). Based on its mode of occurrence,
516 pyrite appears to be syngenetic. Its crystallization is likely associated with pH shifts in the micro-
517 environment during and after coal formation. While the limited presence of pyrite does not strongly
518 support a conclusion in favor of marine incursion, their intermittent occurrence in the sample
519 column suggests a shifting micro-environment within the swamp.

520 Dolomite (S3/B4) and siderite (S5/B3, S5/B4) are not found together in the same sample; rather,
521 each dominates the mineral assemblage in separate samples, with one being dominated by siderite
522 and little to no dolomite (S5/B3), and vice versa. Based on the present mineralogical investigation,
523 the authors suggest that the coal-bearing heterolithic units of the Barakar Formation were likely
524 deposited in a marginal marine environment. Coastal lagoons or salt marshes, separated from the
525 open sea by a barrier, may have experienced periodic seawater intrusion driven by fluctuations in
526 relative sea level.

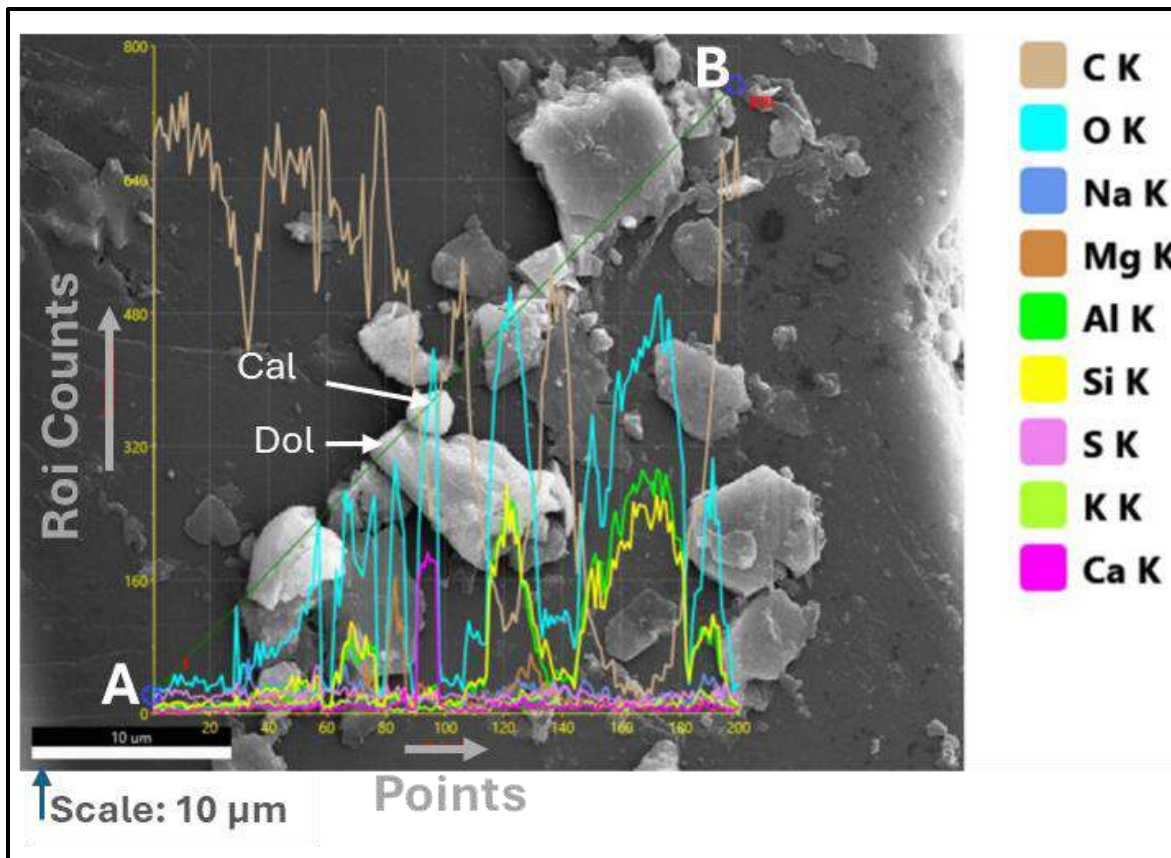
527

528

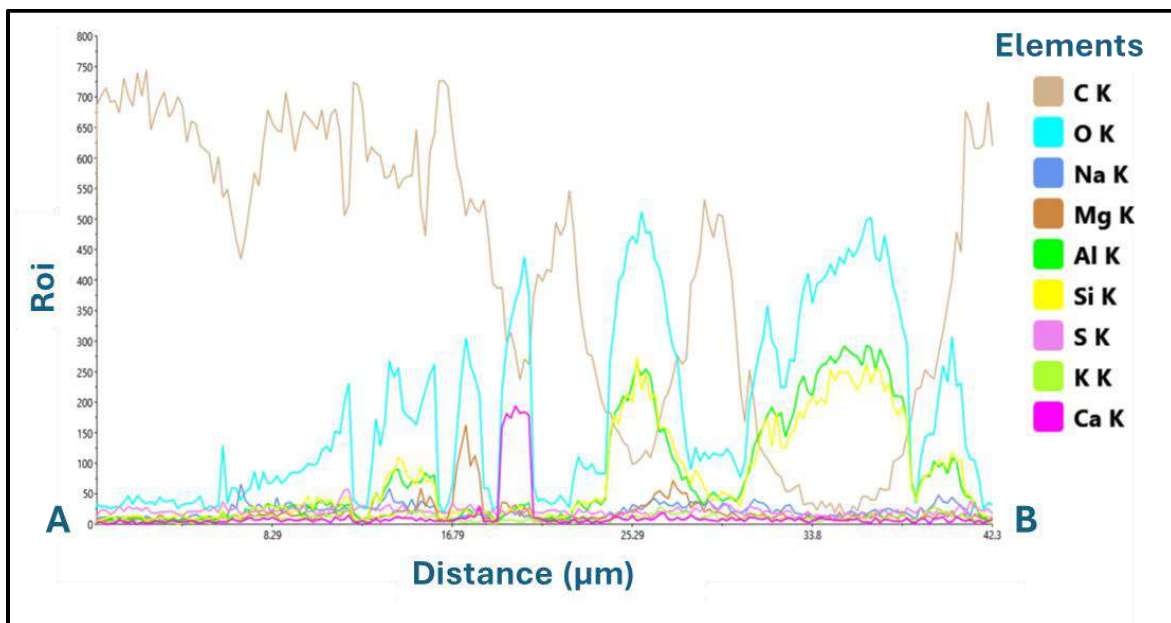
529

530

531

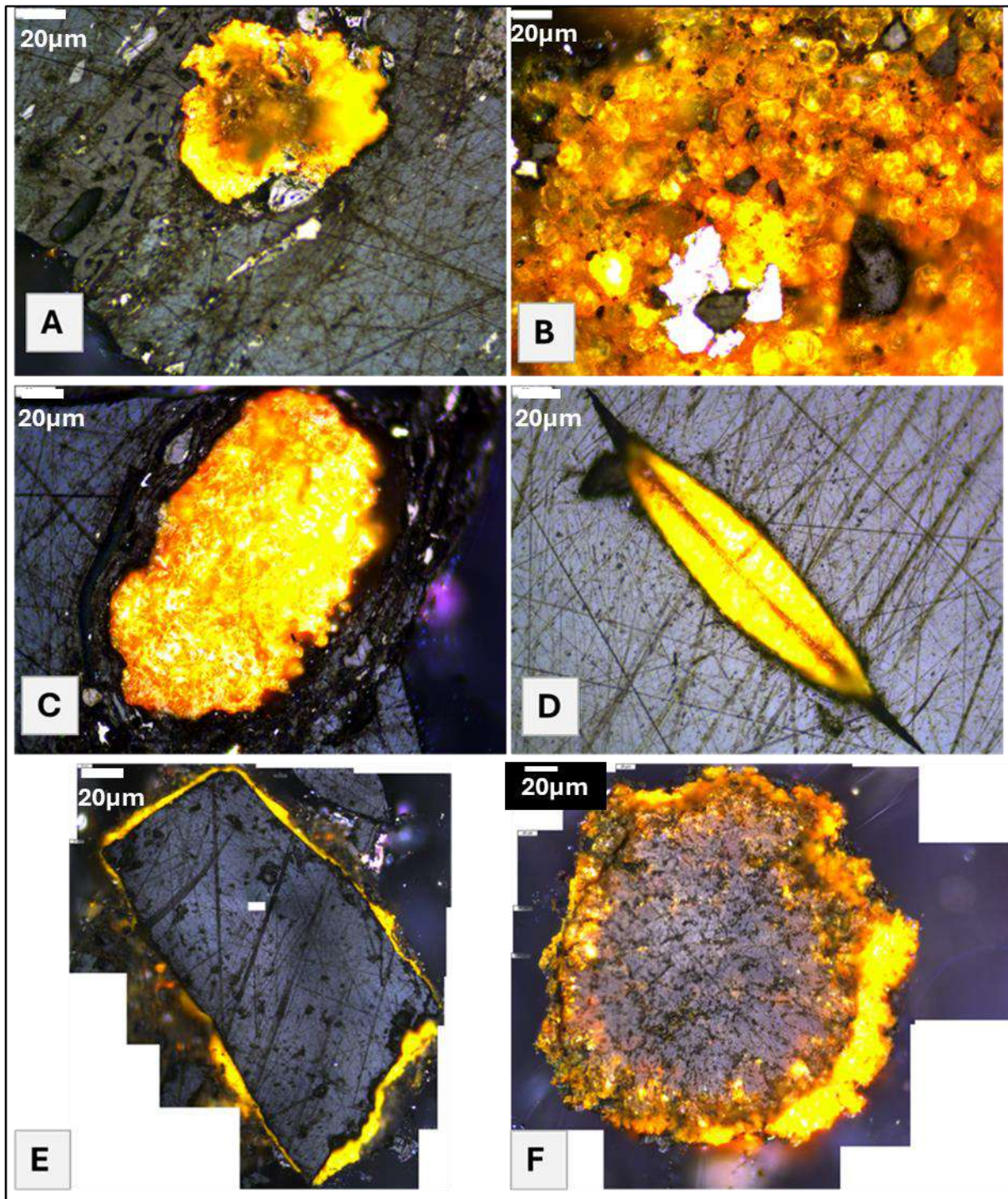


532



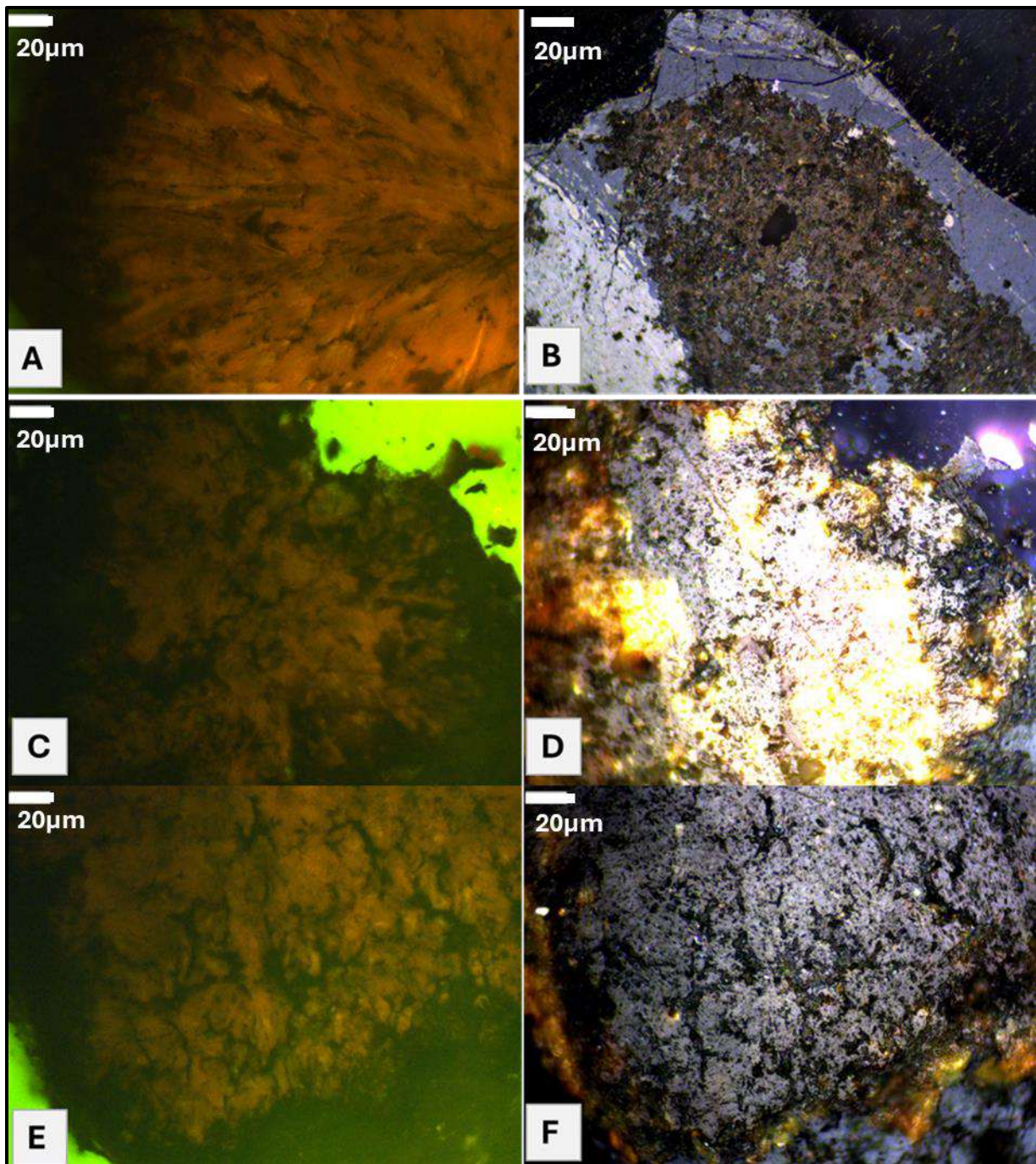
533

534 **Figure 18:** Line scan across line A and B, and corresponding spectra depicting different elements
 535 (Cal- Calcite, Dol- Dolomite), using SEM EDS profiling.



536

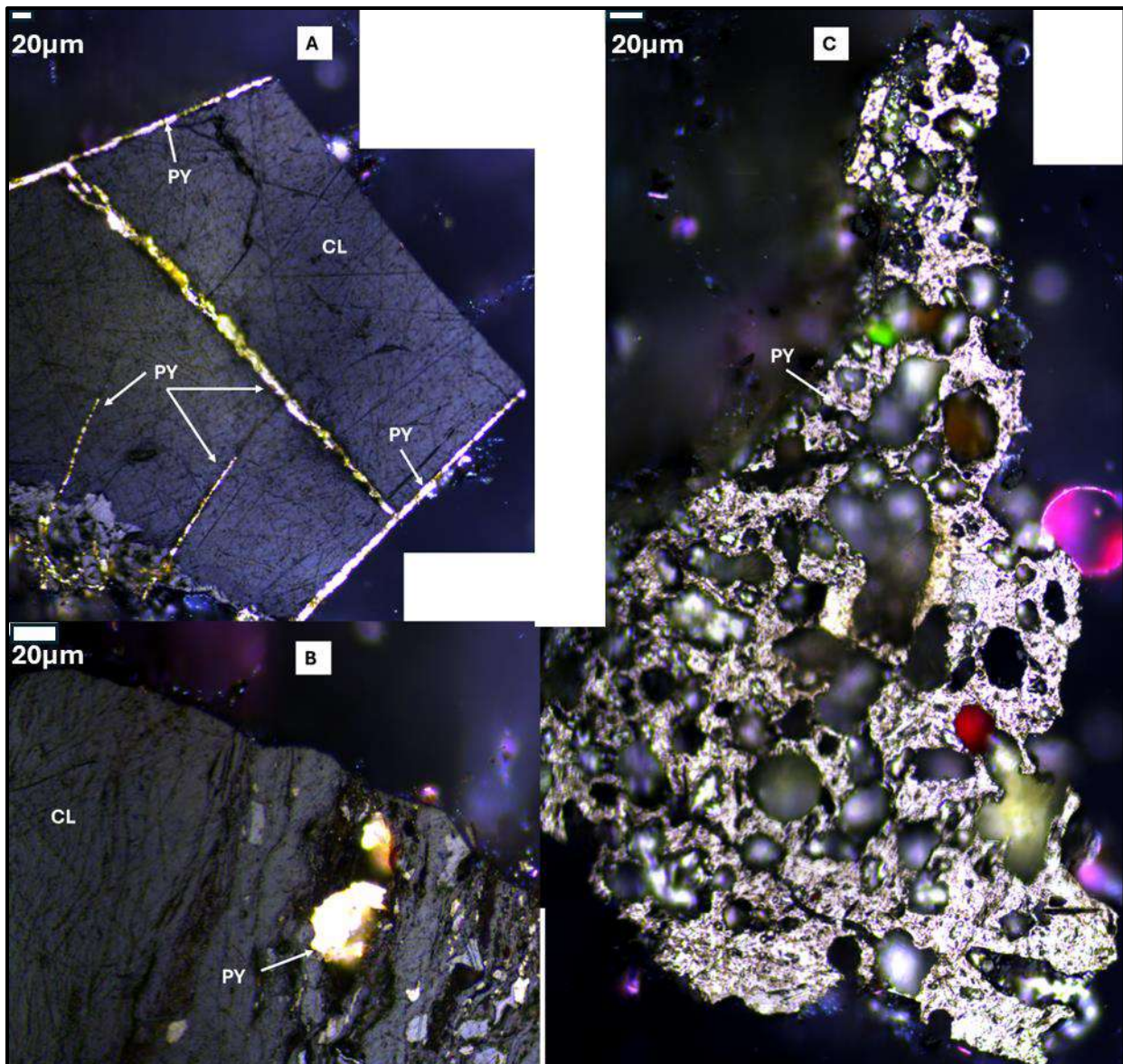
537 **Figure 19:** Coal micro-petrography image of **A.** Fe bearing Calc nodule precipitated on
538 collotelinite, **B.** Calc nodule in cluster, **C.** Calcite precipitated on collotelinite, **D.** Calcite filling
539 the elliptical crack in collotelinite, **E.** Euhedral collotelinite embedded in carbonate, and **F.** Siderite
540 nodule



541

542 **Figure 20:** Coal micro-petrography: A., C., and E. are images of siderite in fluorescent (Blue light)
543 with typical radiating structures in the nodules, and B., D., and F. are images of siderite nodule in
544 white light.

545



546

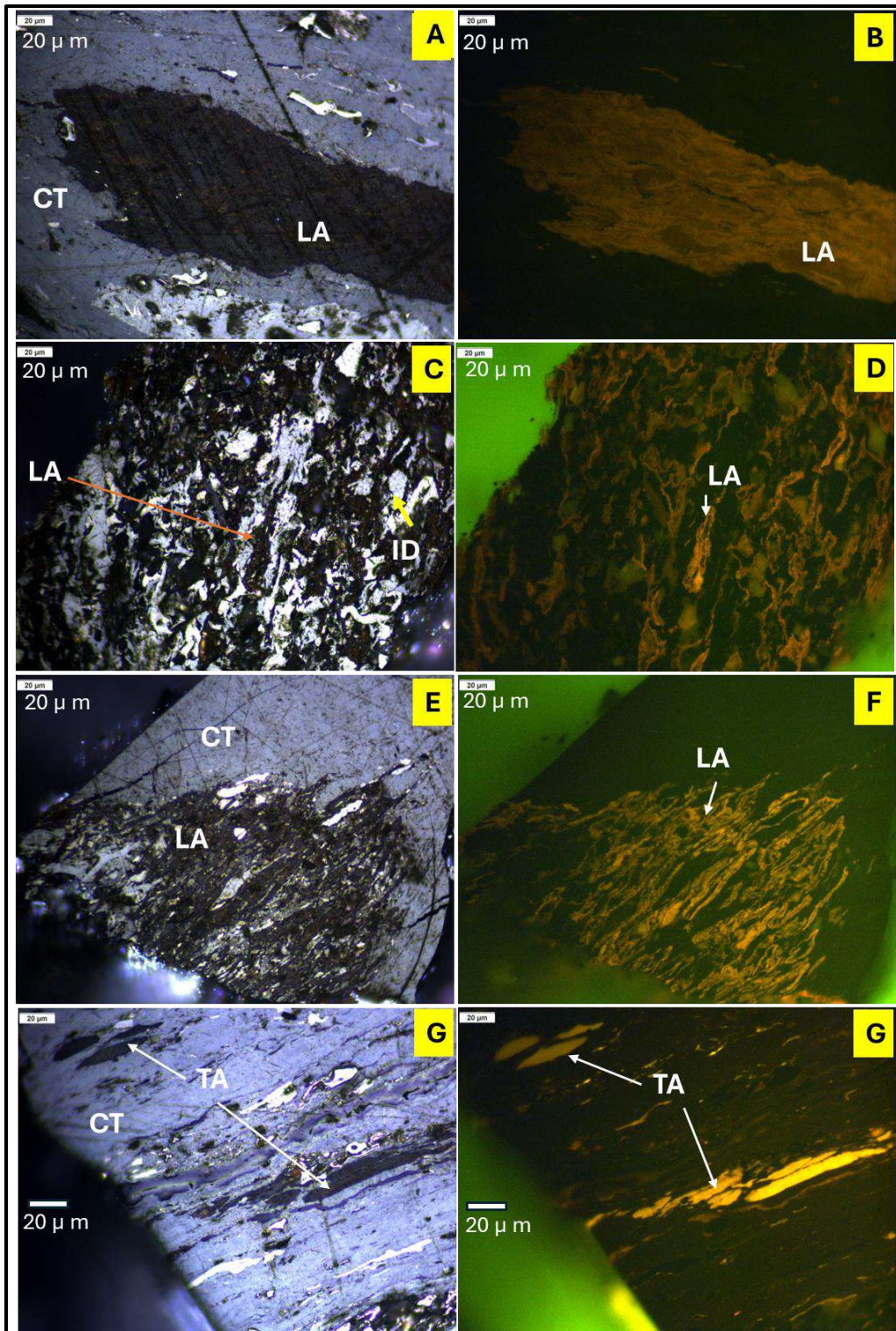
547 **Figure 21:** Coal micro-petrography: A. Collotelinite (CL) cracks filled with pyrite, B. Irregular
 548 pyrite (PY) crystal developed on collotelinite, and C. Encrustations of pyrite on the cell lumens in
 549 fusinite.

550 **4.4 Organic micro-petrographic evidence:**

551 Coal samples for the study area are dominated by Vitrinite followed by Inertinite and Liptinite
 552 group of macerals. The collotelinite is the most abundant sub-maceral, followed by Vitrodetrinite
 553 and Collodetrinite among the vitrinite group. Among Inertinite, Fusinite is most abundant followed
 554 by Semifusinite, Inertodetrinite, Sclerotinite and Macrinite. Micrinite were also present at several

555 locations. A wide variety of liptinite macerals were observed, among which Sporinite, Cutinite,
556 and Alginite are abundantly present. A rare occurrence of Suberinite was discovered from Seam 6.
557 Megasporinite and Fluorinite were also present in several samples.

558 The abundance of alginite in the limited coal samples suggests that the mire developed under
559 subaqueous conditions. Out of the two alginite types identified, lamalginite was more prevalent
560 than telalginite. Telalginite consists of discrete algal bodies, both colonial and unicellular, such as
561 Botryococcus, Tasmanites, and Gloeocapsomorpha (a primitive blue-green algae). In contrast,
562 lamalginite comprises benthonic or pelagic lamellar algae (green or blue green) that occur as finely
563 laminated bands, interbedded with mineral matter either finely or coarsely (Singh and Singh 2004).
564 According to Misra et al. (1998), the presence of alginite in coal and lignite deposits indicates a
565 mixed marine environment, typically nearshore settings (Misra et al. 1998). They further noted
566 that the mode of occurrence, frequency, and preservation state of alginite reflect seasonal
567 paleoenvironmental fluctuations, particularly variations between oxidizing and reducing
568 conditions during the accumulation of vegetal matter (Misra et al. 1998). The coal seam is
569 associated with heterolithic units 3 and 5, where alginite is frequently observed as a liptinite sub-
570 maceral (Figure 22). This suggests that at least these units developed under marine-influenced
571 conditions. The maceral analysis aligns well with geochemical data, both clearly indicating that
572 heterolithic units 3 and 5 were affected by marine transgression.



573

574 **Figure 22:** Micro-photograph A., C., E., and G. under white incident light, and B., D., F., and G.
 575 under blue incident light where, LA=Lamalginite, TA=Telalginate, CT=Collotelinite, ID=
 576 Inertodetrinite, coal sample from seam 3 (heterolithic unite 3) and 5 (heterolithic unite 5).

577 **5 Depositional Model:**

578 The Gondwana basins of India preserve a nearly 200 Ma long geological archive within Peninsular
 579 India. Initially formed as sag basins, they later transitioned into fault-controlled systems due to
 580 widespread tectonic reactivations, mainly linked to pan-Gondwanan geodynamic events. The
 581 sedimentary fill is largely siliciclastic and was primarily deposited in continental environments.
 582 However, distinct marine signatures are evident within the Early and middle Permian sequences
 583 across several Gondwana basins. Detailed investigations of the Indian basins indicate that
 584 sedimentation within the Gondwana Basins was shaped by a dynamic interaction of tectonic
 585 faulting, sea-level fluctuations, and climatic variations (Mukhopadhyay et al. 2010).

586 Talchir Formation exposed in the northwestern part of the West Bokaro basin, has already been
 587 established as a glaciogenic deposition with marine influence at the top (Sengupta; et al. 1999). In
 588 contrast, the overlying Karharbari Formation shows no evidence of marine influence and is
 589 interpreted as a fluvio-lacustrine deposit (Bhattacharya et al. 2005). The HLU, representing the
 590 middle to upper part of the Barakar Formation and covering the major portion of the study area,
 591 appears to have been deposited in a marginal marine environment, as revealed by the present multi-
 592 proxy approach. This interpretation is supported by field studies, geochemical proxies, mineral
 593 and macerals assemblage of coal samples.

594 Geochemical markers in the studied coal samples suggest intermittent marine or brackish water
 595 influence during peat accumulation. The CaO/MgO ratio (ranging from 0 to 3.44, with a mean of
 596 1.51) aligns with values reported for marine-influenced coal deposits. Additionally, the
 597 MgO/Al₂O₃ ratio further supports marine influence, as MgO enrichment is characteristic of such
 598 environments. The log (K₂O/ Al₂O₃) vs. log (MgO/ Al₂O₃) plot confirms that the sediments were
 599 deposited under marine conditions. These findings indicate that the coal seams experienced
 600 multiple episodes of marine transgression or contributions from algal remains during their
 601 formation. Geochemical proxies, including Sr/Ba and Th/U ratios, indicate that the Barakar
 602 Formation experienced a dynamic depositional environment influenced by fluctuating seawater,
 603 brackish water, and freshwater conditions. The Sr/Ba ratio (0.25 to 1.12, mean 0.6) suggests
 604 variable salinity levels, with HLU-3 deposited under full marine inundation, while HLU-1, HLU-
 605 5, and HLU-6 represent transitional brackish settings. Similarly, the Th/U ratio (0.93 to 4.78, mean
 606 2.53) confirms brackish to saline conditions, supporting a marine transgression-regression cycle.

607 Cross-plot analyses further reinforce this interpretation, highlighting periodic marine incursions
608 that shaped the depositional environment of the Early Permian Barakar coals.

609 The presence of authigenic carbonates (Figure 19), including dolomite (Figure 18) and siderite, in
610 the studied coal samples suggests deposition in a marginal marine environment. Dolomite
611 formation indicates periodic marine influence, likely through seawater infiltration into coastal peat
612 swamps, while siderite rich coal (Figure 20) deposits typically associated with freshwater
613 conditions, low sulfur content, absence of sulfate-rich seawater and sulfide ions, and strongly
614 reducing environments (Vassilev et al. 2010). In contrast, they may also get deposited on salt
615 marshes e.g. Norfolk coast, UK. Their mutually exclusive occurrence suggests fluctuating
616 depositional conditions, influenced by sea-level changes. Limited pyrite (Figure 21) occurrence
617 further supports intermittent marine incursions. Overall, the coal-bearing heterolithic units of the
618 Barakar Formation were likely deposited in a coastal lagoon or salt marsh setting, periodically
619 affected by seawater intrusion. The existence of alginite maceral (Figure 22), a transformational
620 product of algae, suggests deposition in a stagnant water condition in a peat swamp environment,
621 likely within a supratidal salt marsh (Figure 24).

622 Sedimentological studies exhibit subtidal to supratidal facies, influenced by intermittent
623 fluctuations of wave energy, ranging from strong to weak, due to open marine storms, and at least
624 at two interval fluvial systems prevailed and resulted in the deposition of two thick trough cross
625 stratified sandstone locally named Dumarbera and Parsatoli Sandstone (Figure 5,13 and 14). The
626 coexistence of wave ripples and tidalites (Figure 10, 11, and 23B) in the HLU suggests an
627 environment where low-energy wave and storm processes interacted with tidal currents. These
628 conditions favored the deposition of fine- to medium-grained sandstones and heterolithic facies,
629 typical of tidal flats, with sedimentary structures reflecting shifting energy conditions. Further, at
630 least five coarsening upward sequences have been reported from the HLU-5 and 6 exposed under
631 quarry no 18 D (Figure 23A), which exhibits tidal bundles, where coal/shale/siltstone present at
632 the bottom of the sequence represents supratidal condition, sandstone- siltstone rhythmites
633 represents intertidal and sandstone represents subtidal condition (Figure 23B). Typically, coal
634 swamps formed due to marine regression, in this case they developed as a result of marine
635 transgression. Similar to the current scenario in the North Sea, the advancing sea pushes the rising
636 groundwater table landward, leading to the formation of new swamp belts. Tidal flat or coastal

637 marine swamps, in particular, become inundated by the sea during transgressive events (Taylor et
638 al. 1998).

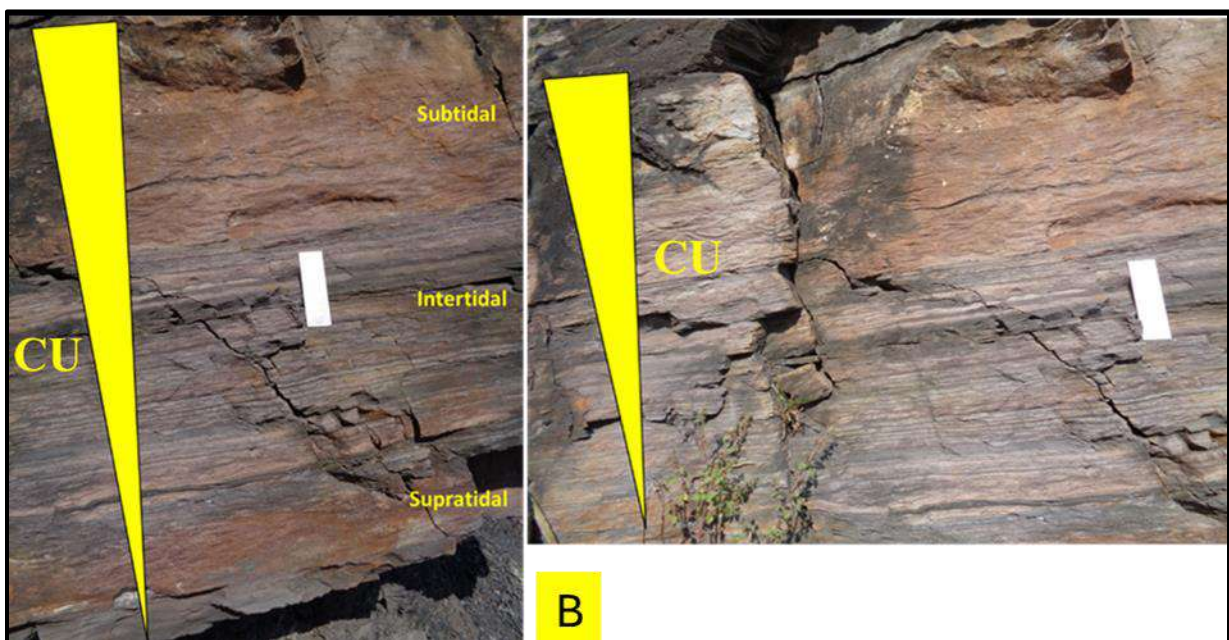
639 During the transgressive phase, the landward migration of the shoreline resulted in a coarsening-
640 upward sequence (Figure 23 A, 24). This is observed in the case of the HLU, where coal and coaly
641 shales present at the base were deposited in a supratidal marsh environment (Figure 23 B). The
642 middle part of the sequence, characterized by rhythmic interbedding of siltstone and shale,
643 represents an intertidal setting, whereas the overlying sandstone reflects subtidal conditions
644 (Figure 23 B). Accordingly, HLU-1 to HLU-4 are interpreted to have been deposited during a
645 transgressive phase over a tidal flat. The Dumarbera Sandstone, a trough cross-bedded sandstone
646 unit, was likely deposited by meandering or braided streams that developed over the supratidal
647 flats during a regressive phase. A renewed marine transgression is marked by the deposition of
648 HLU-5 and HLU-6, followed by the Parsatoli Sandstone unit, which represents another regressive
649 phase. A more extensive marine transgression subsequently led to the deposition of the Barren
650 Measures Formation, as previously demonstrated by Bhattacharya and Banerjee (2015) (Figure
651 25) (Bhattacharya and Banerjee 2015).

652 The Bokaro Basin, a sub-basin within the larger Damodar Basin, lies between regions where
653 marine influence during the Early to Middle Permian has already been established, from the
654 underlying Talchir Formation and overlying Barren Measures above (Bhattacharya and Banerjee
655 2015; Bhattacharya and Mukherjee 2020). Surrounding basins such as Rajmahal and Raniganj to
656 the northeast and east, respectively; and Karanpura, Rajhara, Ramgarh, up till Satpura basin to the
657 west, have also revealed evidence of marine conditions during Barakar sedimentation (Gupta 1999;
658 Chakraborty et al. 2003; Ghosh et al. 2004; Goswami 2008; Bhattacharjee et al. 2018; Mathews et
659 al. 2020; Bhattacharya et al. 2021, 2012a; Pillai et al. 2023).. Even within the West Bokaro Basin
660 itself, marine signatures have been identified at the transition from the upper Barakar to the Barren
661 Measures (Pathak et al. 2024). However, a definitive record of marine incursion during the Barakar
662 deposition in this basin remained unresolved. The present study addresses this gap by documenting
663 clear evidence of marine influence during Barakar sedimentation in the West Bokaro Basin. This
664 contribution helps delineate a near-continuous marine incursion pathway-extending from the
665 Khemgaon, Sikkim corridor through Rajmahal and Raniganj, reaching as far west as the Satpura

666 basin, indicating a sustained marine connection across Gondwana basins during Barakar
 667 deposition.



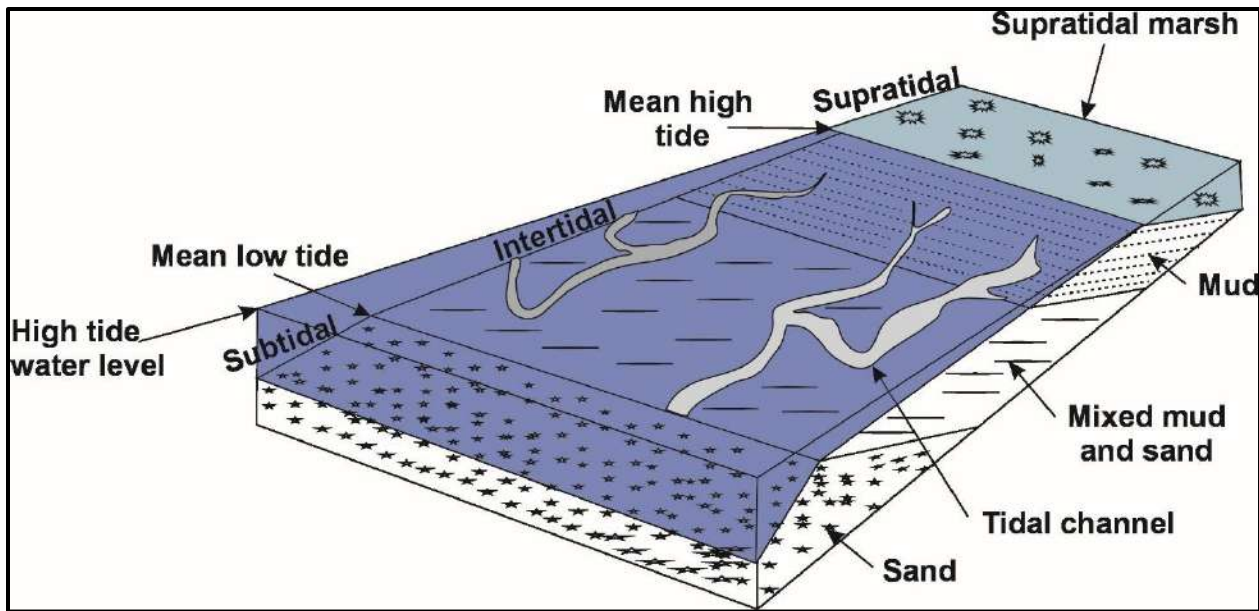
668



669

670 **Figure 23 A.** Heterolithic coal bearing unit near Quarry no. 18D, (HLU-5 and 6, CU=Coarsening
 671 upward), **B.** Closeup view of coarsening upward tidal bundle.

672



673

674 **Figure 24:** Coexistence of wave ripples with tidalites indicate low-energy wave/storm interference
675 with tidal currents. after (Boggs 2006).

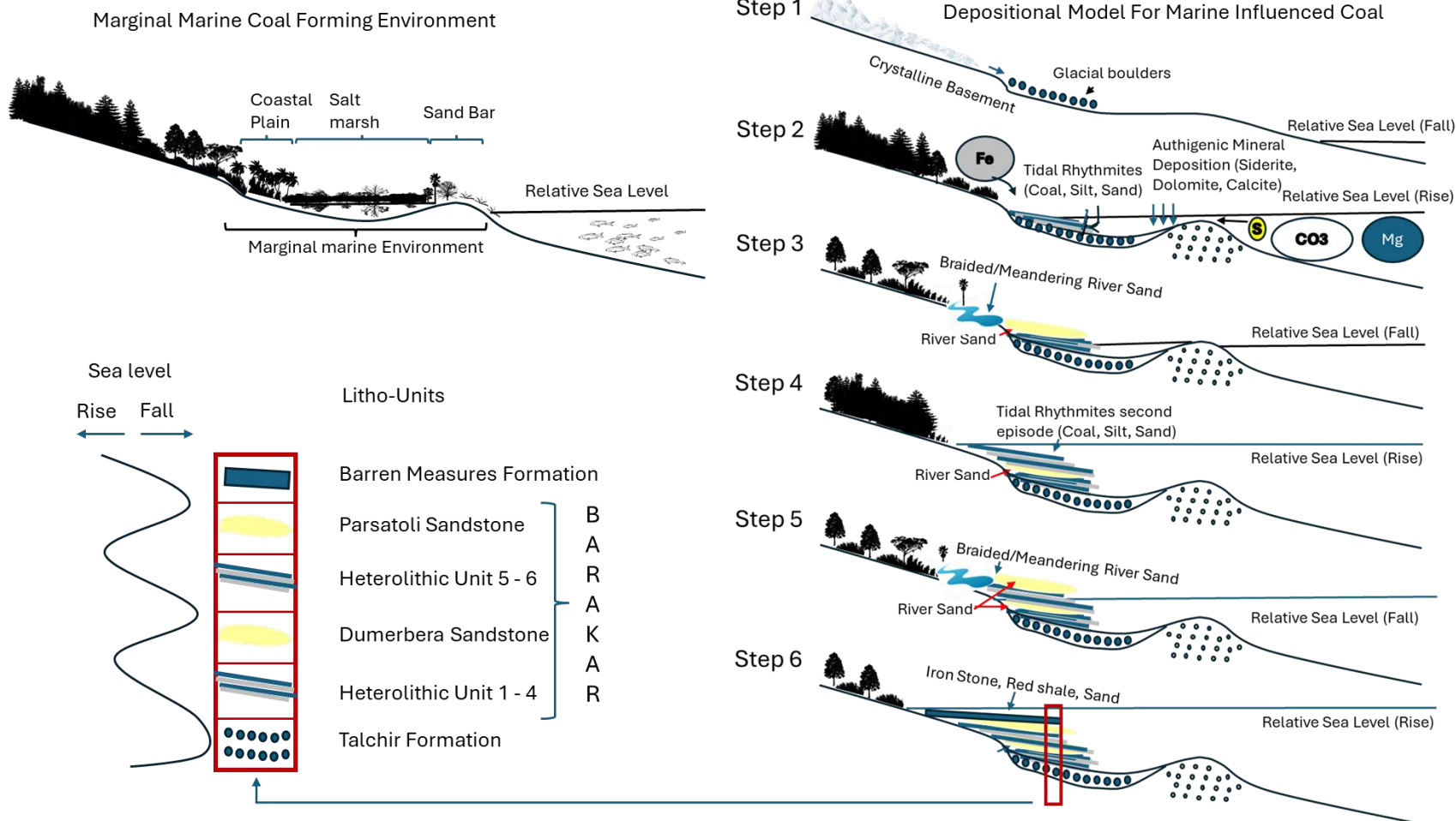


Figure 25: Depositional model for marine influenced coal-bearing heterolithic units of Barakar Formation, Near Ara-Dumerbera, from West Bokaro basin.

6 Conclusion

This depositional model indicates an influence of dynamic coastal environment where tidal and wave interactions played a crucial role in sediment distribution and stratigraphic architecture during the deposition of upper part of the Barakar Formation in the West Bokaro Basin. Evidence suggests that the peat-forming swamps of the Barakar Formation evolved atop supratidal salt marshes. The coal-bearing HLUs of the part of middle to upper Barakar Formation were deposited during multiple episodes of relatively minor marine transgressions. One in the middle of these HLUs and another toward the end of Barakar deposition, a sudden shift toward regression is evident by the deposition of the Dumerbera Sandstone unit and Parsatoli Sandstone unit. This was followed by a significant marine transgression, marking the onset of the Barren Measure Formation, characterized by ironstone-dominated deposits. Integrating previous studies on the Barren Measure Formation in the West Bokaro Basin, it can be inferred that marginal marine conditions in the study area developed earlier than previously reported. The present study establishes definitive evidence of marine influence during Barakar sedimentation in the West Bokaro Basin, thereby confirming a near-continuous marine incursion pathway extending from the Khemgaon-Sikkim corridor through Rajmahal and Raniganj to as far west as the Satpura Basin. This highlights a sustained marine connection across multiple Gondwana basins during the Barakar sedimentation.

Abbreviations:

CU- Coarsening upward

CT- Collotelinite

E- East

ESE- East Southeast

HLU- Heterolithic Unit

ICCP- International Committee for Coal and Organic Petrology

ID - Inertodetrinite

LA- Lamalginit

N- North

NNW- North Northwest

SEM-EDS- Scanning electron microscopy–energy dispersive spectroscopy

TA- Telalginite

XRF- X-ray Fluorescence

References

Ahokas, J.M., J.P. Nystuen, and A.W. Martinius. 2014. “Stratigraphic signatures of punctuated rise in relative sea-level in an estuary-dominated heterolithic succession: Incised valley fills of the Toarcian Ostreaelv Formation, Neill Klinter Group (Jameson Land, East Greenland).” *Marine and Petroleum Geology* 50:103–129. Available at: <http://dx.doi.org/10.1016/j.marpetgeo.2013.11.001>.

Ameh, E.G. 2019. “Geochemistry and multivariate statistical evaluation of major oxides, trace and rare earth elements in coal occurrences and deposits around Kogi east, Northern Anambra Basin, Nigeria.” *International Journal of Coal Science and Technology* 6(2):260–273. Available at: <https://doi.org/10.1007/s40789-019-0247-4>.

Arthur, M., and B. Sageman. 1994. “Marine Shales: Depositional Mechanisms and Environments of Ancient Deposits.” *Annual Review of Earth and Planetary Sciences* 22(1):499–551.

Bann, K.L., C.R. Fielding, J.A. MacEachern, and S.C. Tye. 2004. “Differentiation of estuarine and offshore marine deposits using integrated ichnology and sedimentology: Permian Pebbley Beach Formation, Sydney Basin, Australia.” *Geological Society Special Publication* 228:179–211.

Bhattacharjee, J., K.K. Ghosh, and B. Bhattacharya. 2018. “Petrography and geochemistry of sandstone–mudstone from Barakar Formation (early Permian), Raniganj Basin, India: Implications for provenance, weathering and marine depositional conditions during Lower Gondwana sedimentation.” *Geological Journal* 53(3):1102–1122.

Bhattacharya, B., S. Bandyopadhyay, S. Mahapatra, and S. Banerjee. 2012a. “Record of tide-wave influence on the coal-bearing Permian Barakar Formation, Raniganj Basin, India.” *Sedimentary Geology* 267–268:25–35. Available at: <http://dx.doi.org/10.1016/j.sedgeo.2012.05.006>.

Bhattacharya, B., S. Bandyopadhyay, S. Mahapatra, and S. Banerjee. 2012b. “Record of tide-wave influence on the coal-bearing Permian Barakar Formation, Raniganj Basin, India.” *Sedimentary Geology* 267–268:25–35. Available at: <http://dx.doi.org/10.1016/j.sedgeo.2012.05.006>.

Bhattacharya, B., and P.P. Banerjee. 2015. "Record of Permian Tethyan transgression in eastern India: A reappraisal of the Barren Measures Formation, West Bokaro Coalfield." *Marine and Petroleum Geology* 67:170–179. Available at: <http://dx.doi.org/10.1016/j.marpetgeo.2015.05.008>.

Bhattacharya, B., J. Bhattacharjee, S. Banerjee, T. Roy, and S. Bandyopadhyay. 2021. "Palaeogeographic implications of ichnotaxa assemblages from early Permian fluvio-marine Barakar Formation, Raniganj Basin, India." *Journal of Earth System Science* 130(1).

Bhattacharya, H.N., A. Chakraborty, and B. Bhattacharya. 2005. "Significance of transition between Talchir Formation and Karharbari Formation in Lower Gondwana basin evolution - A study in West Bokaro Coal basin, Jharkhand, India." *Journal of Earth System Science* 114(3):275–286.

Bhattacharya, H.N., and A. Mukherjee. 2020. "Soft-sediment deformation structures in a Permo-carboniferous glacio-marine setting, Talchir Formation, Dudhi Nala, India." *Journal of Earth System Science* 129(1).

Birks, H.H., and H.J.B. Birks. 2006. "Multi-proxy studies in palaeolimnology." *Vegetation History and Archaeobotany* 15(4):235–251.

Boggs Sam. 2006. Principles of Sedimentology and Stratigraphy Fourth Edi.

Borch, T., R. Kretzschmar, A. Skappler, P. Van Cappellen, M. Ginder-Vogel, A. Voegelin, and K. Campbell. 2010. "Biogeochemical redox processes and their impact on contaminant dynamics." *Environmental Science and Technology* 44(1):15–23.

Cao, Y., F. Diao, and H. Zou. 2022. "Depositional Paleoenvironments and Implications on the Occurrence of the Shahejie Formation Source Rock in the Langgu Sag, Bohai Bay Basin." *Frontiers in Earth Science* 10(June).

Chakraborty, C., S.K. Ghosh, and T. Chakraborty. 2003. "Depositional record of tidal-flat sedimentation in the Permian coal measures of central India: Barakar Formation, Mohpani coalfield, Satpura Gondwana basin." *Gondwana Research* 6(4):817–827.

Chatterjee, S., and N. Hotton. 1986. "The paleoposition of India." *Journal of Southeast Asian Earth Sciences* 1(3):145–189.

Collins, D.S., H.D. Johnson, and C.T. Baldwin. 2020. "Architecture and preservation in the fluvial to marine transition zone of a mixed-process humid-tropical delta: Middle Miocene Lambir Formation, Baram Delta Province, north-west Borneo" C. Fielding, ed. *Sedimentology* 67(1):1–46. Available at: <https://onlinelibrary.wiley.com/doi/10.1111/sed.12622>.

Cumberland, S.A., G. Douglas, K. Grice, and J.W. Moreau. 2016. "Uranium mobility in organic matter-rich sediments: A review of geological and geochemical processes." *Earth-Science Reviews* 159:160–185. Available at: <http://dx.doi.org/10.1016/j.earscirev.2016.05.010>.

Dim, C.I.P., K.M. Onuoha, I.C. Okwara, I.A. Okonkwo, and P.O. Ibemesi. 2019. "Facies analysis and depositional environment of the Campano – Maastrichtian coal-bearing Mamu Formation

in the Anambra Basin, Nigeria.” *Journal of African Earth Sciences* 152(January 2018):69–83. Available at: <https://doi.org/10.1016/j.jafrearsci.2019.01.011>.

Dutt, A.B. 2019. *Structure and Tectonics of Bokaro and Adjoining Subsidiary Basins* 1st ed. Elsevier Inc. Available at: <http://dx.doi.org/10.1016/B978-0-12-815218-8.00007-8>.

FU, J., S. LI, L. XU, and X. NIU. 2018. “Paleo-sedimentary environmental restoration and its significance of Chang 7 Member of Triassic Yanchang Formation in Ordos Basin, NW China.” *Petroleum Exploration and Development* 45(6):998–1008.

Ghosh, S. kumar, C. Chakraborty, and T. Chakraborty. 2004. “Combined tide and wave influence on sedimentation of Lower Gondwana coal measures of central India: Barakar Formation (Permian), Satpura basin.” *Journal of the Geological Society* 161(1):117–131. Available at: <https://www.lyellcollection.org/doi/10.1144/0016-764902-077>.

Gingras, M.K., J.A. MacEachern, S.E. Dashtgard, M.J. Ranger, and S.G. Pemberton. 2016. “The significance of trace fossils in the McMurray formation, Alberta, Canada.” *Bulletin of Canadian Petroleum Geology* 64(2):233–250.

Goswami, S. 2008. “Marine influence and incursion in the Gondwana basins of Orissa, India: A review.” *Palaeoworld* 17(1):21–32.

Gupta, A. 1999. “Early Permian Palaeoenvironment in Damodar Valley Coalfields, India: An Overview.” *Gondwana Research* 2(2):149–165.

Gupta, R., and H.D. Johnson. 2001. “Characterization of heterolithic deposits using electrofacies analysis in the tide-dominated Lower Jurassic Cook Formation (Gullfaks field, offshore Norway).” *Petroleum Geoscience* 7(3):321–330.

ICCP. 2001. “New inertinite classification (ICCP System 1994).” *Fuel* 80(4):459–471.

ICCP. 1998. “The new vitrinite classification (ICCP system 1994): International Committee for Coal and Organic Petrology (ICCP).” *Fuel* 77(5):349–358.

ISO:7404-5. 2004. “METHODS FOR THE PETROGRAPHIC ANALYSIS OF BITUMINOUS COAL AND ANTHRACITE.”

Jenkins, R.J.F., C.H. Ford, and J.G. Gehling. 1983. “The ediacara member of the rawnsley quartzite: The context of the ediacara assemblage (late precambrian, flinders ranges).” *Journal of the Geological Society of Australia* 30(1–2):101–119.

Jha, Y.N., and H.N. Sinha. 2022. “Acritarchs - Palynomorphs from the Barren Measures Formation of West Bokaro Coalfield: Implications to Depositional Environment.” *Journal of Geosciences Research* 7(2):166–171.

Leclair, S.F. 2002. “Preservation of cross-strata due to the migration of subaqueous dunes: An experimental investigation.” *Sedimentology* 49(6):1157–1180.

Li, D., R. Li, Z. Zhu, X. Wu, F. Liu, B. Zhao, J. Cheng, and B. Wang. 2018. "Elemental characteristics and paleoenvironment reconstruction: a case study of the Triassic lacustrine Zhangjiatan oil shale, southern Ordos Basin, China." *Acta Geochimica* 37(1):134–150.

Lin, C.Y., A. V. Turchyn, A. Krylov, and G. Antler. 2020a. "The microbially driven formation of siderite in salt marsh sediments." *Geobiology* 18(2):207–224.

Lin, C.Y., A. V. Turchyn, A. Krylov, and G. Antler. 2020b. "The microbially driven formation of siderite in salt marsh sediments." *Geobiology* 18(2):207–224.

Mahato, O., and P.K. Srivastava. 2023. "Quantitative Mineralogical Analysis and Study of Morphology and Thermal Characteristics of Rock Samples of Dudhi Nala and Bokaro River." *Oriental Journal Of Chemistry* 39(5):1373–1378.

Martinius, A.W., I. Kaas, A. NSS, G. Helgesen, J.M. Kjrefjord, and D.A. Leith. 2001. "Sedimentology of the heterolithic and tide-dominated tilje formation (Early Jurassic, Halten Terrace, Offshore Mid-Norway)." *Norwegian Petroleum Society Special Publications* 10(C):103–144.

Martinius, A.W., P.S. Ringrose, C. Brostrøm, C. Elfenbein, A. Næss, and J.E. Ringås. 2005. "Reservoir challenges of heterolithic tidal sandstone reservoirs in the Halten Terrace, mid-Norway." *Petroleum Geoscience* 11(1):3–16.

Mathews, R.P., S.S.K. Pillai, M.C. Manoj, and S. Agrawal. 2020. "Palaeoenvironmental reconstruction and evidence of marine influence in Permian coal-bearing sequence from Lalmatia Coal mine (Rajmahal Basin), Jharkhand, India: A multi-proxy approach." *International Journal of Coal Geology* 224(April):103485. Available at: <https://doi.org/10.1016/j.coal.2020.103485>.

Melnyk, S., and M.K. Gingras. 2020. "Using ichnological relationships to interpret heterolithic fabrics in fluvio-tidal settings." *Sedimentology* 67(2):1069–1083.

Misra, B.K., B.D. Singh, and A. Singh. 1998. "Maceral alginite in Indian coals and lignites: Its significance and influence." *Journal of Palaeosciences* 47(1984):37–49.

Mukhopadhyay, G., S.K. Mukhopadhyay, M. Roychowdhury, and P.K. Parui. 2010. "Stratigraphic correlation between different Gondwana Basins of India." *Journal of the Geological Society of India* 76(3):251–266.

Navale, G.K.B., and R. Saxena. 1989. "An appraisal of coal petrographic facies in Lower Gondwana (Permian) coal seams of India." *International Journal of Coal Geology* 12(1–4):553–588. Available at: <https://linkinghub.elsevier.com/retrieve/pii/0166516289900657>.

Ogbe, O.B., and J. Osokpor. 2021. "Depositional facies, sequence stratigraphy and reservoir potential of the Eocene Nanka Formation of the Ameki Group in Agu-Awka and Umunya, southeast Nigeria." *Heliyon* 7(1):e05846. Available at: <https://doi.org/10.1016/j.heliyon.2020.e05846>.

Olariu, C., R.J. Steel, M.I. Olariu, and K. Choi. 2015. *Facies and architecture of unusual fluvial-tidal channels with inclined heterolithic strata: Campanian Neslen Formation, Utah, USA* 1st ed. Elsevier B.V. Available at: <http://dx.doi.org/10.1016/B978-0-444-63529-7.00011-0>.

Pathak, A., B. Bhattacharya, M. Banerjee, and A. Bhattacharya. 2024. "Sequence stratigraphic reappraisal of the nature of transition between two lithostratigraphic units (formations) – A study from the Permian Lower Gondwana succession, West Bokaro Basin, Eastern India." *Marine and Petroleum Geology* 162(October 2023):106749. Available at: <https://doi.org/10.1016/j.marpetgeo.2024.106749>.

Pickel, W., J. Kus, D. Flores, S. Kalaitzidis, K. Christianis, B.J. Cardott, M. Misz-Kennan, S. Rodrigues, A. Hentschel, M. Hamor-Vido, P. Crosdale, and N. Wagner. 2017. "Classification of liptinite – ICCP System 1994." *International Journal of Coal Geology* 169:40–61.

Pillai, S.S.K., M.C. Manoj, R.P. Mathews, S. Murthy, M. Sahoo, A. Saxena, A. Sharma, S. Pradhan, and S. Kumar. 2023. *Lower Permian Gondwana sequence of Rajhara (Daltonganj Coalfield), Damodar Basin, India: floristic and geochemical records and their implications on marine ingressions and depositional environment*. Springer Netherlands. Available at: <https://doi.org/10.1007/s10653-023-01517-8>.

Pye, K. 1984. "SEM analysis of siderite cements in intertidal marsh sediments, Norfolk, England." *Marine Geology* 56(1–4):1–12.

Pye, K., J.A.D. DICKSON, N. SCHIAVON, M.L. COLEMAN, and M. COX. 1990. "Formation of siderite-Mg-calcite-iron sulphide concretions in intertidal marsh and sandflat sediments, north Norfolk, England." *Sedimentology* 37(2):325–343.

Quamar, M.F., B. Thakur, A. Sharma, K. Kumar, P. Tiwari, A. Tiwari, N. Prasad, J. Srivastava, B. Phartiyal, M.C. Manoj, I.H. Roy, P.N. Saraf, K. Prasanna, N. Ali, I. Khan, S. Pandey, and A. Trivedi. 2024. "Multiproxy studies on the spatially distinct surface samples to reconstruct palaeoecology and palaeoclimate from the Core Monsoon Zone of India." *Journal of the Palaeontological Society of India* 69(1):21–36.

Raja Rao, C.S. 1987. "Coalfields of India."

Ray, S., and T. Chakraborty. 2002. "Lower Gondwana fluvial succession of the PenchKanhan valley." 151:243–271.

Reineck, HE., and IB. Singh. 1980. *Depositional Sedimentary Environments* Second.

Ringrose, P., K. Nordahl, and R. Wen. 2005. "Vertical permeability estimation in heterolithic tidal deltaic sandstones." *Petroleum Geoscience* 11(1):29–36.

S. M. Casshyap, R.C.T. 1987. "PbV36_59.pdf." *The Palaeobotanist* 36:59–66.

S. Sengupta; A. Chakraborty; and H. N. Bhattacharya; 1999. "Fossil Polyplacophora (Mollusca) from Upper Talchir Sediments of Dudhi Nala, Hazaribagh, Bihar." *Journal of the Geological Society of India* 54:523–527. Available at: <https://doi.org/10.17491/jgsi/1999/540509>.

Schieber, J. 1989. "Facies and origin of shales from the mid-Proterozoic Newland Formation, Belt Basin, Montana, USA." *Sedimentology* 36(2):203–219.

Schroeter, N., J.L. Toney, S. Lauterbach, J. Kalanke, A. Schwarz, S. Schouten, and G. Gleixner. 2020. "How to Deal With Multi-Proxy Data for Paleoenvironmental Reconstructions: Applications to a Holocene Lake Sediment Record From the Tian Shan, Central Asia." *Frontiers in Earth Science* 8(September):1–18.

Scott, A.C. 1987. "Coal and coal-bearing strata: Recent advances and future prospects." *Geological Society Special Publication* 32(32):1–6.

Singh, B.D., and A. Singh. 2004. "Observations on Indian Permian Gondwana coals under fluorescence microscopy: An overview." *Gondwana Research* 7(1):143–151.

Sinha, S.K., and S.D. Gupta. 2020. "Missing Coal Seam between East and West Bokaro near Lugu Hill of Damodar Basin, India: A Geological Model." *Journal of the Geological Society of India* 96(3):298–307.

Spiro, B.F., J. Liu, S. Dai, R. Zeng, D. Large, and D. French. 2019. "Marine derived $^{87}\text{Sr}/^{86}\text{Sr}$ in coal, a new key to geochronology and palaeoenvironment: Elucidation of the India-Eurasia and China-Indochina collisions in Yunnan, China." *International Journal of Coal Geology* 215(October):103304. Available at: <https://doi.org/10.1016/j.coal.2019.103304>.

Srikanta Murthy. 2017. "Late Permian palynomorphs from the West Bokaro." *The Palaeobotanist* 66:201–209.

Srivastava, M.K., K. Kishor, M. Nath, and A.K. Singh. 2024. "Inorganic geochemical attributes of Jaintia Hills coals, India: Implications for paleo-depositional conditions." *Kuwait Journal of Science* 51(3):100227. Available at: <https://doi.org/10.1016/j.kjs.2024.100227>.

Srivastava, M.K., K. Kishor, A.K. Singh, S. Mukherjee, and S.K. Bharti. 2025. "Tectonically deformed coal: Focus on microstructures & implications for basin evolution." *Marine and Petroleum Geology* 172(November 2024):107223. Available at: <https://doi.org/10.1016/j.marpetgeo.2024.107223>.

Stach, E., M. Mackowsky, M. Teichmuller, G. Taylor, D. Chandra, and R. Teichmuller. 1982. *Textbook of Coal Petrology*.

Taylor, G.H., M. Teichmüller, A. Davis, C.F.K. Diessel, R. Littke, and P. Robert. 1998. *Organic Petrology*.

Tewari, R.C., R.N. Hota, and W. Maejima. 2012. "Fluvial architecture of Early Permian Barakar rocks of Korba Gondwana basin, eastern-central India." *Journal of Asian Earth Sciences* 52:43–52. Available at: <http://dx.doi.org/10.1016/j.jseaes.2012.02.009>.

Tewari, R.C., and W. Maejima. 2010. "Origin of gondwana basins of peninsular India." *Journal of Geosciences* 53(July):43–49.

Tiwari, A.K., P.K. Singh, S. Chandra, and A. Ghosh. 2016. "Assessment of groundwater level fluctuation by using remote sensing and GIS in West Bokaro coalfield, Jharkhand, India." *ISH Journal of Hydraulic Engineering* 22(1):59–67.

Tiwari, A.K., P.K. Singh, and M.K. Mahato. 2016. "Hydrogeochemical investigation and qualitative assessment of surface water resources in West Bokaro coalfield, India." *Journal of the Geological Society of India* 87(1):85–96.

Vassilev, S. V., and C.G. Vassileva. 1996. "Occurrence, abundance and origin of minerals in coals and coal ashes." *Fuel Processing Technology* 48(2):85–106.

Vassilev, S. V., C.G. Vassileva, D. Baxter, and L.K. Andersen. 2010. "Relationships between chemical and mineral composition of coal and their potential applications as genetic indicators. Part 2. Mineral classes, groups and species." *Geologica Balcanica* 39(3):43–67.

Vassilev, S., C. Vassileva, D. Baxter, and L. Andersen. 2010. "Relationships between chemical and mineral composition of coal and their potential applications as genetic indicators. Part 2. Mineral classes, groups and species." *Geologica Balcanica* 39(3):43–67.

Venkatachala, B.S., and R.S. Tiwari. 1987. "Lower Gondwana marine incursions: periods and pathways." *Journal of Palaeosciences* 36:24–29.

Wei, S., M. Hu, S. He, W. Yang, Q. He, Q. Cai, and P. Li. 2023. "Sedimentary Environment Interpretation and Organic Matter Enrichment of the Lower Cambrian Shuijingtuo Shale in the Yichang Slope, South China: Insight from Sedimentary Geochemical Proxies with Major/Trace Elements." *Journal of Marine Science and Engineering* 11(10).

Wei, W., and T.J. Algeo. 2020. "Elemental proxies for paleosalinity analysis of ancient shales and mudrocks." *Geochimica et Cosmochimica Acta* 287:341–366. Available at: <https://doi.org/10.1016/j.gca.2019.06.034>.

Willis, B.J., and H. Tang. 2010. "Three-dimensional connectivity of point-bar deposits." *Journal of Sedimentary Research* 80(5–6):440–454.

Zuo, X., C. Li, J. Zhang, G. Ma, and P. Chen. 2020. "Geochemical characteristics and depositional environment of the Shahejie Formation in the Binnan Oilfield, China." *Journal of Geophysics and Engineering* 17(3):539–551.